Accepted Manuscript

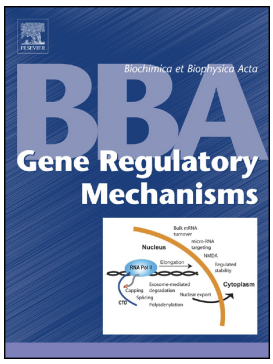

Dynamic transcriptional control of macrophage miRNA signature via inflammation responsive enhancers revealed using a combination of next generation sequencing-based approaches

Zsolt Czimmerer, Attila Horvath, Bence Daniel, Gergely Nagy, Ixchelt Cuaranta-Monroy, Mate Kiss, Zsuzsanna Kolostyak, Szilard Poliska, Laszlo Steiner, Nikolas Giannakis, Tamas Varga, Laszlo Nagy

PII: S1874-9399(17)30177-3
DOI: doi:10.1016/j.bbagrm.2017.11.003
Reference: BBAGRM 1190

To appear in:

Received date: 26 May 2017
Revised date: 23 October 2017
Accepted date: 9 November 2017

Please cite this article as: Zsolt Czimmerer, Attila Horvath, Bence Daniel, Gergely Nagy, Ixchelt Cuaranta-Monroy, Mate Kiss, Zsuzsanna Kolostyak, Szilard Poliska, Laszlo Steiner, Nikolas Giannakis, Tamas Varga, Laszlo Nagy , Dynamic transcriptional control of macrophage miRNA signature via inflammation responsive enhancers revealed using a combination of next generation sequencing-based approaches. The address for the corresponding author was captured as affiliation for all authors. Please check if appropriate. Bbagrm(2017), doi:10.1016/j.bbagrm.2017.11.003

This is a PDF file of an unedited manuscript that has been accepted for publication. As a service to our customers we are providing this early version of the manuscript. The manuscript will undergo copyediting, typesetting, and review of the resulting proof before it is published in its final form. Please note that during the production process errors may be discovered which could affect the content, and all legal disclaimers that apply to the journal pertain.

ACCEPTED MANUSCRIPT

BBAGRM_2017_107 REVISED_2

Dynamic transcriptional control of macrophage miRNA signature via inflammation responsive enhancers revealed using a combination of next generation sequencing-based approaches

Zsolt Czimmerer[1, 6], Attila Horvath[1, 6], Bence Daniel[2, 6], Gergely Nagy[1, 5], Ixchelt Cuaranta-Monroy[1], Mate Kiss[1], Zsuzsanna Kolostyak[1], Szilard Poliska[3], Laszlo Steiner[4], Nikolas Giannakis[1, 4], Tamas Varga[1], Laszlo Nagy[1, 2, 5, 7]

[1] Department of Biochemistry and Molecular Biology, Faculty of Medicine, University of Debrecen, Debrecen, Hungary

[2] Sanford-Burnham-Prebys Medical Discovery Institute, Genomic Control of Metabolism Program, 6400 Sanger Road, Orlando, FL 32827 USA

[3] Genomic Medicine and Bioinformatic Core Facility, Department of Biochemistry and Molecular Biology, Faculty of Medicine, University of Debrecen, Debrecen, Hungary

[4] UD-Genomed Medical Genomic Technologies Ltd., Debrecen, Hungary

[5] MTA-DE „Lendület" Immunogenomics Research Group, University of Debrecen, Debrecen, Hungary

[6] These authors contributed equally to this work.

[7] Corresponding author:

lnagy@sbpdiscovery.org

407-745-2150

ACCEPTED MANUSCRIPT

Abstract

MicroRNAs are important components of the post-transcriptional fine-tuning of macrophage gene expression in physiological and pathological conditions. However, the mechanistic underpinnings and the cis-acting genomic factors of how macrophage polarizing signals induce miRNA expression changes are not well characterized. Therefore, we systematically evaluated the transcriptional basis underlying the inflammation-mediated regulation of macrophage microRNome using the combination of different next generation sequencing datasets. We investigated the LPS-induced expression changes at mature miRNA and pri-miRNA levels in mouse macrophages utilizing a small RNA-seq method and publicly available GRO-seq dataset, respectively. Next, we identified an enhancer set associated with LPS-responsive pri-miRNAs based on publicly available H3K4 mono-methylation-specific ChIP-seq and GRO-seq datasets. This enhancer set was further characterized by the combination of publicly available ChIP and ATAC-seq datasets. Finally, direct interactions between the miR-155-coding genomic region and its distal regulatory elements were identified using a 3C-seq approach. Our analysis revealed 15 robustly LPS-regulated miRNAs at the transcriptional level. In addition, we found that these miRNA genes are associated with an inflammation-responsive enhancer network. Based on NFκB-p65 and JunB transcription factor binding, we showed two distinct enhancer subsets associated with LPS-activated miRNAs that possess distinct epigenetic characteristics and LPS-responsiveness. Finally, our 3C-seq analysis revealed the LPS-induced extensive reorganization of the pri-miR-155-associated functional chromatin domain as well as chromatin loop formation between LPS-responsive enhancers and the promoter region. Our genomic approach successfully combines various genome-wide datasets and allows the identification of the putative regulatory elements controlling miRNA expression in classically activated macrophages.

Keywords: pri-miRNA, inflammation, macrophage, enhancer, chromatin looping

ACCEPTED MANUSCRIPT

ACCEPTED MANUSCRIPT

Highlights

- Next generation sequencing-based approaches were applied to investigate the transcriptional regulation of miRNA expression.
- 22 transcriptionally regulated miRNAs were identified in LPS-activated macrophages.
- LPS-regulated pri-miRNAs are associated with 52 induced and 25 repressed enhancers.
- 2 distinct LPS-activated enhancer subsets can be distinguished based on inflammatory responsiveness, NFkB and AP-1 binding and distinct epigenetic characteristics.
- The architecture of pri-miR-155-associated topological domain undergoes LPS-induced spatial reorganization.

ACCEPTED MANUSCRIPT

ACCEPTED MANUSCRIPT

1. Introduction

MicroRNAs (miRNAs) are the most studied class of the small non-coding RNAs [1, 2]. They are well characterized components of the post-transcriptional fine-tuning of gene expression in mammals and participate in the regulation of embryonic development, cellular differentiation as well as disease progression [3-6]. MiRNA genes are located in both intergenic regions and intronic/exonic regions of protein-coding genes in the genome [2]. Their primary transcripts, pri-miRNAs, are usually transcribed by RNA polymerase II [7], although RNA polymerase III-transcribed pri-miRNAs have also been described [8]. Pri-miRNAs are processed in nuclear and cytoplasmic steps by RNase III enzymes Drosha and Dicer [2]. Mature miRNAs are loaded into RNA-induced silencing complex (RISC) and generally recognize the 3' untranslated regions (3'UTR) of their target mRNAs [9]. RISC-incorporated miRNAs act as negative regulators of gene expression via induction of target mRNA degradation or inhibition of protein synthesis [6, 9, 10].

Despite the fact that several regulatory mechanisms of miRNA expression are described at different levels of miRNA biogenesis, including transcription, processing and transport (reviewed in [11]), the transcriptional control of miRNA expression under different physiological and pathological conditions remains poorly understood. Although a few studies demonstrated the involvement of distinct tissue or signal-specific transcription factors, the number of published genome-wide miRNA transcriptional studies are limited. This is mainly due to technical difficulties and certain biological features of pri-miRNAs including (i) rapid processing and low copy number of pri-miRNAs, (ii) inadequate annotation of pri-miRNA genes, and (iii) lack of integrated genomic and bioinformatics approaches [12-16]. The *in silico* combination of genome sequence and ditag expression data may provide insight into the transcript structure of pri-miRNAs but this information alone is not sufficient to determine the cell type- and internal/external signal-dependent regulation of pri-miRNA expression [17]. Next generation sequencing (NGS) technologies including Global Run On and sequencing (GRO-seq), Chromatin Immunoprecpitation and sequencing (ChIP-seq) and bisulfite sequencing provide valuable information about the transcriptional regulation of miRNAs [18-22]. By using GRO-seq, 322 expressed and 119 17β-estradiol-regulated pri-miRNAs have been identified in the estrogen-receptor α-positive MCF-7 human breast cancer cell line [18]. Combined analysis of histone modifications and DNA methylation at miRNA promoters proved to be a useful, but limited approach to determine the epigenetic regulation of miRNA expression in colorectal cancer cells and monocyte-derived dendritic cells [20, 21]. ChIP-seq-based detection of active histone mark H3K4m3 alone or in combination with RNA polymerase II binding proved to be suitable for identifying active pri-miRNA promoter regions [19, 21, 23, 24]. However, our understanding about the involvement of additional cis-regulatory components in the control of miRNA transcription is far from complete.

It has become evident in recent years that the long-range interaction between promoters and distal-acting enhancers is necessary for cell type-specific and/or signal-dependent expression of coding and non-coding transcripts [25]. The integration of different NGS methods including Assay for Transposase-Accessible Chromatin with high-throughput sequencing (ATAC-seq), GRO-seq, ChIP-seq of general enhancer mark H3K4m1 and chromosome conformation capture techniques are suitable tools to identify enhancer networks and functional promoter-enhancer interactions in different cellular systems (reviewed in [26, 27]). Nonetheless, our current knowledge about cell type or signal-specific enhancer networks in the regulation of pri-miRNA transcriptome is limited to only a handful of examples [28, 29]. Therefore a more thorough and better integrated epigenomic approach is needed in order to

ACCEPTED MANUSCRIPT

identify (1) transcription units of pri-miRNAs, (2) transcription start sites (TSS) and promoters, (3) proximal and distal enhancers and long-range interactions regulating miRNA gene expression. Macrophages display substantial functional heterogeneity, they are essential for the maintenance of tissue homeostasis and play critical roles in the regulation of inflammatory response against invading microbial pathogens as well as the resolution of inflammation. In addition, they are involved in the pathophysiology of chronic inflammatory diseases and tumor development [30, 31]. Inflammatory macrophage phenotype is triggered by pathogen-derived molecules such as lipopolysaccharide (LPS) and inflammatory cytokines including interferon gamma (IFNγ) or tumor necrosis factor alpha (TNFα) through the activation of the Janus kinase (JAK)/signal transducer and activator of transcription (STAT1) axis or the activator protein 1 (AP-1) and nuclear factor kappa-light-chain-enhancer of activated B cells (NFkB) signaling pathways [32, 33]. The functional properties associated with inflammatory signal-induced macrophage activation require tight regulation of the inflammation-specific gene expression program at the transcriptional and post-transcriptional levels [31]. It has been shown that, along with changes in mRNA transcription, the miRNA signature of macrophages is also modulated following LPS stimulation or microbial pathogen infections [34-37]. Inflammation responsive miRNAs proved to be important post-transcriptional regulators in controlling the function of macrophages, either promoting the pro-inflammatory macrophage activation or inhibiting the overwhelming inflammatory response [38-45]. Despite the well known miRNA-associated functions during inflammatory macrophage activation, the mechanistic background of inflammation-dependent regulation of miRNA expression is poorly understood.

Here we provide a complex NGS-based approach combining small RNA-seq, GRO-seq, ChIP-seq, ATAC-seq and 3C-seq methods to unravel the transcriptional basis of inflammation-induced changes in the macrophage miRNome. Our strategy has led to the annotation of inflammation-responsive enhancers to microRNA genes and validated the physical interactions between the LPS-activated pri-miR-155 promoter and its enhancers.

2. Materials and methods

2.1. Animals:

Wild-type (C57BL/6J) mice were housed under minimal disease conditions and the experiments were carried out under institutional ethical guidelines and licenses. Animal experiments in the Nagy laboratory were carried out with protocols approved by the Institutional Review Board of the University of Debrecen (file numbers: 120/2009/DE MAB and 21/2011/DE MAB).

2.2. Materials:

LPS (*Salmonella enterica* serotype minnesota Re 595) was obtained from Sigma Aldrich.

2.3. Differentiation of bone marrow-derived macrophages:

Bone marrow was isolated from 8-12 weeks old male mice. Isolation and differentiation were completed as described earlier [46]. Isolated bone marrow-derived cells were differentiated for 6 days in the presence of L929 supernatant. Cells were polarized on the 6th day of the differentiation with LPS (100 ng/ml) for the indicated period of time.

ACCEPTED MANUSCRIPT

2.4. Small RNA-sequencing and data analysis:

Small RNA-sequencing libraries were generated from 1 μg of total RNA using TruSeq Small RNA Sample Preparation Kit (Illumina) according to manufacturer's protocol. Briefly, after ligation of 3' and 5' RNA adapters, reverse transcription was performed to synthesize cDNA and then using Illumina specific index adapter primers, cDNA was amplified. The amplified library was excised from 6% Novex TBE PAGE gel (Invitrogen) and after purification the libraries were quantified by Qubit fluorometer and checked on BioAnalyzer 2100 using DNA1000 chip (Agilent Technologies). Single read 50bp sequencing was performed on HiScanSQ instrument (Illumina). Small RNA-seq samples were aligned by novoalign (with –r Random and –m options) to mm10 genome assembly (GRCm38.p1.) and converted into BAM files with SAMtools [47, 48]. The Rsubread and edgeR packages were used to quantify and infer the statistically significant miRNAs using mature miRNA collection from MirBase (v21), respectively. CPM (counts per million) scores were normalized by using TMM method. For the downstream analysis only the expressed miRNAs (CPM>=10 at least in two samples) and significantly changed (p-value<=0.05 and FDR <= 0.1) miRNAs were used.

2.5. Real-time quantitative PCR:

Total RNA was isolated from cells using Tri Reagent (MRC) according to manufacturer's protocol. For quantification of mRNAs and pri-miRNAs reverse transcription was performed by using High-Capacity cDNA Reverse Transcription Kit (Applied Biosystems). RT primers for mature miRNAs were supplied by Applied Biosystems. Transcript quantification was performed by quantitative real-time RT (reverse transcriptase) PCR (polymerase chain reaction) using SYBR Green assays (selfmade assays). qPCR assays and primer sequences are listed in Supplementary Table 1.

2.6. GRO-seq and ChIP-seq and ATAC-seq data analysis:

Primary analysis of the raw reads was carried out using our ChIP-seq analysis command line pipeline [49]. Briefly, Burrows-Wheeler Alignment Tool (BWA, [50]) was used to align the reads to mm10 genome assembly (GRCm38.p1.) with default parameters [47]. MACS2 [51] was used for predicting transcription factor peaks (q-value<=0.01) and findPeaks.pl (with '-size 1000' and '-minDist 2500' options) for histone regions with option '-style histone' [52]. Artifacts were removed using the ENCODE blacklist (ENCODE Cons.) [53]. This pipeline is available upon request. Predicted peaks were sorted by average coverage (RPKM, Reads Per Kilobase per Million mapped reads) calculated by DiffBind v1.0.9 [54]. Intersections, subtractions and merging of the predicted peaks were made with BedTools [55]. Proportional Venn diagrams were generated with VennMaster [56]. Genome coverage files (bedgraph files) for visualization were generated by makeUCSCfile.pl and then converted into tdf files using igvtools with 'toTDF' option [57]. *De novo* motif discovery was performed on the 100 bp vicinity of the peak summits using findMotifsGenome.pl from HOMER. Integrative Genomics Viewer (IGV2.3, Broad Institute) was used for data browsing [57] and creating representative snapshots. Normalized tag counts for Meta histograms and RD plots were generated by annotatePeaks.pl with '-ghist' and '-hist 25' options from HOMER and then visualized by Java TreeView or R using ggplot2 [58]. GRO-seq transcripts were predicted by findPeaks.pl with '-style groseq' option of HOMER (with parameters minBodySize=1000, maxBodySize=80000, tssFold=5, bodyFold=1.5 endFold=6.5) and merged with known gene bodies within a window of 1000bp in a strand specific manner. Finally to make the prediction

ACCEPTED MANUSCRIPT

of TSSs of predicted transcripts more precise they were split by the union of control and LPS treated H3K4m3 regions (3000bp distance between features allowed for features to be merged) dealing with the cases when there is more than active promoter regions on the same transcript. TSS predictions from FANTOM5 data set aligned to mm9 was converted to mm10 genome using liftOver [59].

2.7. Domain prediction:

Raw ChIP-seq reads of 47 CTCF and 42 Cohesin (RAD21, SMC1/3 or SA1/2) samples were downloaded from the Sequence Read Achive of NCBI and processed by our ChIP-seq analysis command line pipeline [49]. Peaks determined by MACS2 [51] were filtered by score (≥10) and the blacklist of ENCODE [53]. Consensus CTCF peak summits were defined as the average genomic location of at least two summits within 51 bp. Consensus peak summits for Cohesin were defined in the same manner. Insulator peak summits were determined from those consensus CTCF peak summits that were closer to a consensus Cohesin peak summit than 51 bp. Motif enrichments were determined in two rounds by findMotifsGenome.pl (HOMER) [52] from the 100 bp region around the 5000 most ubiquitous insulator peak summits. After mapping the putative elements matching with the CTCF motif of the first search by annotatePeaks.pl (HOMER), we used those top 5000 regions lacking these hits. Score 6 was set for both CTCF motif matrices, and to filter putative CTCF elements in the case of multiple occurrences at the same region, we preferred those hits following the direction of the CTCF/Cohesin peak location compared to each other [60, 61] and having the highest motif score. Insulators showing clear protein-binding direction without predicted element were also included in domain prediction. Read density (RPKM) of CTCF and RAD21 ChIP-seq derived from bone marrow-derived macrophages was calculated on the 100 bp wide genomic region around insulators, and those regions having an RPKM value exceeding the hundred-thousandth of the summed density of all regions per sample in both samples were selected. The closest insulators showing convergent direction within 1 Mb distance and farther than 1 Kb were assigned to each other and called domains if their coverage showed less than 2-fold difference for both proteins. In the case of overlapping domains, those having the highest insulator coverage were selected. Domains with divergent insulators were determined in a similar manner.

2.8. Enhancer annotation and eRNA expression analysis:

Enhancer transcripts were predicted based on the pool of the sequence reads derived from the (2x4) LPS-treated time-course GRO-seq samples according to our previous work [46]. From nearby enhancers within 1 Kb, those were used in the further analyses showing the highest expression calculated in RPKM. Enhancers were filtered based on their expression level (over 0.5 RPKM in at least one sample per replicate), expression change (at least 1.3 fold change in the same time point(s) in both replicates as compared to time 0) and the overlap with H3K4m1 enrichment upon LPS treatment (according to the region prediction of HOMER). Intergenic H3K4m1/eRNA "double positive" enhancers farther than 1 Kb and within 50 Kb compared to LPS-responsive pri-miRNA TSSs and/or within the predicted domains around the pri-miRNA TSSs and flanked by the highest CTCF/Cohesin peaks were assigned to the associated gene. RPKM values for H3K4m1 enrichment were calculated within the 1 Kb wide region around the annotated enhancers.

ACCEPTED MANUSCRIPT

2.9. ChIP:

ChIP was performed essentially as previously described [46, 62]. The following antibodies were used: P300 (sc-585), PU.1 (sc-352), p65 (sc-372), PolII-pS5 (ab5131) and PolII-pS2 (ab5095). Primer sequences are available upon request. The amount of immunoprecipitated DNA was quantified with Qubit fluorometer (Invitrogen). DNA was applied for qPCR analysis. Primer sequences are listed in Supplementary Table 2.

2.10. 3C-seq and analysis:

Experiments were carried out as previously described (Stadhouders et al., 2013). After the first digestion and ligation the 3C DNA pool was purified with phenol/chloroform/ isoamyl alcohol (25:24:1) (Sigma). Second restriction digestion was performed by using DpnII (NEB) for 16 hours per manufacturer's instruction. Second ligation was performed at 16C for 6 hours with 200U of T4 DNA ligase. DNA was then purified again with phenol/chloroform/isoamyl alcohol (25:24:1) followed by QIAquick gel purification columns (Qiagen). Bait specific inverse PCRs were performed using primers coupled to Universal Illumina adapters and Barcode sequences. Reactions were purified by QIAquick gel purification columns. Amplicon libraries were quantified and qualified by Agilent using DNA 7500 chip cartridge. Primers are available upon request. Amplicon libraries were sequenced on Illumina HiSeq sequencer. Raw reads were demultiplexed using FASTX-Toolkit and then aligned to mm10 genome assembly (GRCm38.p1.) by BWA [50]. Bedgraph and TDF files for visualization were generated as previously described. The R package r3Cseq (pvalue<=0.05) was used to predict the putative interactions [63].

2. 11. Availability of data and materials

Small RNA sequencing and 3C sequencing data were submitted to NCBI SRA depository under accession number PRJNA379555. ChIP-seq data were downloaded from the NCBI GEO depository (GSE38379, GSE16723) and from NCBI SRA depository (accesion number PRJNA194083). GRO-seq data were downloaded from the NCBI GEO depository (GSE60857). ATAC-seq data were downloaded from the NCBI GEO depository (GSE78873). The used genome-wide datasets are collected in Supplementary Table 3.

2.12. Statistical analysis

RT-qPCR and ChIP-qPCR assays were presented as mean +/-SD. We made at least two biological replicates and we performed one-way Anova with Dunnett post-hoc test and results were considered significant with $p < 0.05$.

3. Results

3.1. Characterization of the transcriptional basis of inflammation responsive miRNA signature in macrophages

In order to determine which macrophage-expressed miRNAs are responsive to inflammatory signals, we exposed mouse bone-marrow-derived macrophages (BMDMs) to LPS stimulus

ACCEPTED MANUSCRIPT

for 3 hours and performed small RNA sequencing. We observed that 261 miRNAs were expressed in unstimulated BMDMs (Supplementary Table 4) and 17 miRNAs showed significantly different expression upon LPS treatment (p-value<0.05 and FDR<0.1; 4 downregulated and 13 upregulated; Supplementary Table 5).

To explore the potential regulatory mechanisms controlling LPS-dependent miRNA expression, we identified the pri-miRNA transcripts using the combination of publicly available GRO-seq and H3K4m3-specific (active gene promoter mark) ChIP-seq datasets from control and LPS-activated BMDMs [64, 65]. We detected 518 sense nascent RNA transcripts overlapping with 568 miRNA genes in the absence and/or presence of LPS activation (Supplementary Table 6). 12 of the detected nascent RNA transcripts overlapped with the genes of 17 LPS-regulated miRNAs (Supplementary Table 6). Next, we investigated the genomic location and primary transcript size of inflammation responsive miRNAs. 58% of them were intergenic, while 17% and 25% showed intronic and exonic localization, respectively (Supplementary Figure 1A). Although, the length distribution of pri-miRNAs was very diverse (ranging from 5,6 to 73 Kb) the majority of primary transcripts (9/12) fell within the range of 5,6-20Kb (Supplementary Figure 1B). To investigate the transcriptional or posttranscriptional regulatory effects of LPS, we determined the pri-miRNA expression changes using the same GRO-seq datasets [65]. 15 out of 17 transcribed LPS-responsive miRNAs (3 down-regulated and 12 upregulated) showed similar LPS-mediated expression patterns with their pri-miRNAs (3 down-regulated and 7 up-regulated; 3 LPS-induced pri-miRNAs contained more than one miRNAs) suggesting dominantly transcriptional regulation of miRNA expression in inflammatory macrophages (Figure 1A). For validation purposes, we selected three previously published inflammation-responsive miRNAs, including the LPS-induced miR-155 and miR-147 as well as the LPS-repressed miR-223 (Figure 1B) [38-44]. Time course experiments of LPS stimulation validated the LPS-mediated induction of pri-miR-155 and pri-miR-147 and the suppression of pri-miR-223 expression (Figure 1C).

Taken together, these results indicate that the majority of inflammation responsive miRNAs are regulated at the transcriptional level in BMDMs. Nevertheless, differential regulation of certain pri-miRNAs and mature miRNAs suggests the participation of post-transcriptional regulatory mechanisms.

3.2. Transcription start sites of inflammation responsive pri-miRNAs are associated with general active promoter marks and RNA polymerase II binding

It is well known that specific epigenetic marks including H3K4m3 and H3K27Ac as well as RNA polymerase II (RNAPII) binding are associated with the promoter region of transcriptionally active protein-coding genes [26, 66]. Recently, active promoter-specific H3K4m3 and RNAPII binding has been previously used for the identification of pri-miRNA promoter regions as well [23, 24]. In order to see if inflammation-regulated pri-miRNA genes have similar epigenetic signatures, we analyzed publicly available H3K4m3, H3K27Ac and RNAPII-specific ChIP-seq datasets from both unstimulated and LPS-stimulated BMDMs [64]. As expected, transcriptional start sites (TSSs) of the inflammation-responsive pri-miRNA genes were associated with H3K4m3, H3K27Ac and RNA Pol II enrichments (Figure 1D, Supplementary Figure 1C and data not shown). LPS exposure enhanced the presence of H3K27Ac and RNAPII on the TSSs of LPS-activated pri-miRNAs, including pri-miR-155 and pri-miR-147 (Figure 1D and Supplementary Figure 1C). In contrast, LPS-dependent reduction of H3K27Ac and RNAPII binding were detected at the TSSs of

ACCEPTED MANUSCRIPT

inflammation-repressed pri-miRNA genes such as pri-miR-223, without the alteration of H3K4m3 enrichment (Figure 1D and Supplementary Figure 1C).

Taken together, these findings confirmed that (i) inflammation sensitive miRNA genes have similar epigenetic features as protein-coding genes and (ii) their transcription seems to be dependent on RNAPII.

3.3. LPS-regulated pri-miRNAs are associated with an inflammation-responsive enhancer network

Eukaryotic enhancers associating with protein-coding genes are marked by specific post-translational histone modifications including H3 histone lysine 4 mono- and dimethylation (H3K4m1, H3K4m2) and enhancer RNA (eRNA) expression (Reviewed in [67] and [68]. Enhancers have also been shown to regulate pri-miRNA transcription in many cell types and tissues [28, 29]. These pri-miRNA-associated distal regulatory regions have general enhancer-like characteristics including enhancer-specific H3K4 mono-methylation and eRNA expression [28, 29]. Based on these findings, we aimed to determine whether inflammation-responsive enhancers can be found in the same topologically associated domains with pri-miRNA genes by using publicly available H3K4m1-specific ChIP-seq and GRO-seq datasets [64, 65]. We performed sub-topological domain (sub-TAD) prediction based on mouse BMDM-derived CTCF and Rad21 datasets, utilizing a previously described algorithm [46, 60, 69-71].

As expected, inflammation responsive pri-miRNA genes were associated with H3K4m1 and eRNA "positive" distal regulatory elements (Supplementary Figure 2A, Figure 2A and B). Our global analysis revealed 33 induced and 11 repressed enhancers (Supplementary Figure 2A and Figure 2B) in the sub-TADs of LPS-regulated pri-miRNA genes (Supplementary Figure 2A and Figure2B). Genomic distribution of inflammation regulated enhancers relative to the TSS of pri-miRNAs revealed that 67% (22/33) of activated enhancers showed upstream localization from the corresponding TSSs (Supplementary Figure 2B). In addition, 48% (16/33) of LPS-activated enhancers were located more than 40 Kb from TSSs (Supplementary Figure 2B). LPS-repressed enhancers also showed asymmetric distribution around the TSS, however, 73% (8/11) of them were located within 40 Kb relative to TSS (Supplementary Figure 2B), suggesting that repressive mechanisms more often operate from closer distances compared to the activating ones.

Next, we decided to identify and characterize inflammation responsive enhancers in the annotated sub-TADs of LPS-regulated miR-155, miR-147 and miR-223 genes. We identified 9 and 2 H3K4m1 positive enhancers, exhibiting LPS-induced eRNA expression in the pri-miR-155 and pri-miR-147 sub-TADs, respectively (Figure 2C). On the other hand, the LPS-repressed pri-miR-223 gene was associated with 3 LPS-repressed enhancers (Figure 2C). For all three pri-miRNAs, we selected 2-2 enhancers for the further characterization by measuring LPS-dependent eRNA expression using RT-qPCR. LPS-dependent activation of selected pri-miR-155-associated enhancers correlated with pri-miRNA expression (Figure 1C and 2D). Similarly, elevated eRNA expression was observed at pri-miR-147_+14 Kb and +27Kb enhancers after LPS treatment, followed by induced pri-miR-147 expression (Figure 1C and 2D). However, the examined pri-miR-147-associated enhancers showed different activation kinetics at later time points (12 and 24 hours) of LPS stimulation. The pri-miR-147_+27 Kb enhancer activity showed significant reduction compared to its maximal

ACCEPTED MANUSCRIPT

expression level following 12 and 24 hours of LPS treatment (Figure 2D). In contrast, eRNA expression remained at a high level at the latest (12 and 24 hours) time points after LPS stimulation at pri-miR-147_+14 Kb enhancer (Figure 2D). Finally, the selected pri-miR-223-associated enhancers were repressed significantly as early as 1 hour after LPS stimulation and showed reduced enhancer activities at the 24 hour time point similarly to pri-miR-223 expression (Figure 1C and 2D).

Overall, these results demonstrate that LPS-sensitive miRNA genes are associated with enhancers showing coordinated eRNA expression changes that follow the kinetics of pri-miRNA expression. These results are consistent with studies focusing on mRNA-associated enhancers, thus suggest that enhancers may participate in the transcriptional regulation of LPS-responsive miRNA expression, analogous to mRNAs [72, 73].

3.4. Classification of inflammation responsive pri-miRNA-associated enhancers based on NFkB-p65 binding

Exposure of macrophages to LPS leads to the activation of NFkB and AP-1 transcription factor complexes resulting in dramatic changes in the chromatin structure, epigenome and transcriptome of immune cells [74]. In order to assess the contribution of NFkB and AP-1 transcription factor complexes to the regulation of LPS-responsive pri-miRNAs, we analyzed the binding of NFkB subunit p65 and AP-1 complex member JunB at the LPS-regulated enhancers using publicly available ChIP-seq data [64, 72]. As we expected, NFkB-p65 binding was negligible in unstimulated BMDMs, while LPS stimulation recruited NFkB-p65 to 13961 genomic regions (Supplementary Figure 3A). Conversely, JunB binding was detected at 6497 genomic sites in resting macrophages, and this number increased to 47057 after LPS stimulation (Supplementary Figure 3A). By focusing on the pri-miRNA-associated LPS-activated enhancers, we found that 51,5% (17/33) of them showed NFkB-p65 binding ("$p65^{high}$" enhancers) while the remaining 48,5% (16/33) were not associated with NFkB-p65 binding ("$p65^{low}$" enhancers) (Figure 3A, B and Supplementary Figure 3A). In contrast, we could not detect NFkB-p65 binding at the majority (9/11) of enhancers associated with LPS-repressed pri-miRNAs (Figure 3A, B and Supplementary Figure 3A). We observed that basal and LPS-induced JunB binding was weaker at LPS-activated $p65^{low}$ enhancers compared to $p65^{high}$ enhancers (Figure 3C and Supplementary Figure 3A). Similarly, LPS-repressed enhancers showed low JunB occupancy both in resting and LPS stimulated macrophages (Figure 3C and Supplementary Figure 3A).

As expected, *de novo* motif analysis under NFkB-p65 and JunB peaks revealed significant enrichment of NFkB-p65 and Jun-AP1 motifs (Supplementary Figure 3B and C). Targeted motif discovery at the LPS-responsive pri-miRNAs-associated enhancer subsets showed that both NFkB-p65 and Jun-AP1 motifs were found a higher number at the $p65^{high}$ enhancers compared to the $p65^{low}$ and LPS-repressed enhancers (Figure 3D). Interestingly, Jun-AP1 motif number (30) was higher at $p65^{high}$ enhancers compared to NFkB-p65 motif number (8) despite the fact that LPS-induced JunB and p65 binding were similar (Figure 3B, C, D and Supplementary Figure 3A). Collectively, these results demonstrate that enhancers associated with LPS-activated pri-miRNAs show distinct NFkB-p65 and JunB binding patterns, whereas LPS-repressed enhancers are associated with low NFkB-p65 and JunB binding, indicating the presence of indirect repressive mechanisms.

ACCEPTED MANUSCRIPT

3.5. LPS-activated p65^{high} and p65^{low} pri-miRNA-linked enhancers have different epigenetic characteristics

In order to investigate whether the functional characteristics of inflammation-responsive enhancers are determined by NFkB-p65 and JunB binding, we analyzed publicly available H3K4m1, H3K27Ac and RNAPII-specific ChIP-seq as well as ATAC-seq datasets from unstimulated and LPS-stimulated mouse BMDMs [64, 75]. Interestingly, basal chromatin accessibility was higher at p65^{high} compared to p65^{low} LPS-activated enhancers in unstimulated BMDMs (Figure 4A). Although chromatin accessibility was induced in an LPS-dependent manner at both p65^{high} and p65^{low} enhancers, a greater increase was observed at p65^{high} enhancers compared to p65^{low} enhancers after 6 hours of LPS-stimulation (Figure 4A). In contrast, both basal and LPS-modulated H3K4m1 enrichments were similar at p65^{high} and p65^{low} LPS-activated enhancers (Figure 4B). Furthermore, elevated basal and LPS-induced H3K27Ac enrichment and RNAPII binding were observed at LPS-activated p65^{high} enhancers compared to p65^{low} enhancers (Figure 4C, D and E). As expected, both H3K27Ac and RNAPII enrichment were reduced, while H3K4m1 enrichment and chromatin accessibility were not influenced at LPS-repressed enhancers following LPS stimulation (Figure 2A, Figure 4A, C, D and E).

In order to gain insight into the additional features of NFkB-p65/JunB-dependent and independent activation of inflammation-responsive pri-miRNA-associated enhancers, we selected four p65^{high} enhancers (pri-miR-155_-76Kb, pri-miR-155_-116Kb, pri-miR-155_-92Kb, pri-miR-147_+27Kb) and two p65^{low} enhancers (pri-miR-155_-62Kb, pri-miR-147_+14Kb) for further characterization (Figure 4E). We determined the binding kinetics of NFkB-p65, PU.1 (macrophage lineage-determining transcription factor), P300 (transcriptional co-activator) and RNAPII at the selected enhancers in mouse BMDMs by ChIP-qPCR. LPS-dependent induction of NFkB-p65 binding reached maximal occupancy at 1 hour and it continuously decreased at later time points (6 and 24 hours) (Figure 5). As we expected, p65-binding was weakly detectable at p65^{low} enhancers (Figure 5). In contrast to NFkB-p65 binding, Pu.1-binding showed similar basal levels at p65^{high} and p65^{low} enhancers and all the enhancers showed induced Pu.1 occupancy after 1 hour of LPS stimulation which remained nearly unchanged at later time points (6 and 24 hours) (Figure 5).

Finally, we studied the binding kinetics of p300, transcription initiation-specific RNAPII-pS5 (serine 5 phosphorylated) and elongation-specific RNAPII-pS2 (serine 2 phosphorylated) at the selected enhancers. LPS-induced binding of p300, RNAPII-S5 and S2 proved to be higher at the p65^{high} compared to the p65^{low} enhancers (Figure 5). Interestingly, we observed temporal differences in RNAPII binding between pri-miR-155 and pri-miR-147-associated enhancers. Pri-miR-155-associated enhancers showed rapid RNAPII p-S2 and p-S5 recruitment after 1 hour of LPS stimulation (Figure 5), while pri-miR-147-linked enhancers showed a delayed RNAPII recruitment peaking at 6 hours (Figure 5).

Altogether, our results suggest that NFkB-dependent and independent processes equally participate in the establishment of inflammatory pri-miRNA gene/enhancer signature. Although H3K4m1 enrichment and LPS-dependent PU.1 binding did not show major differences between p65^{low} and p65^{high} enhancers, chromatin accessibility, H3K27Ac enrichment, p300 and RNAPII-binding of activated enhancers positively correlated with the strength of NFkB-p65 and JunB-binding. Finally, the temporal kinetics of RNAPII recruitment upon LPS stimulus showed pri-miRNA locus specificity.

ACCEPTED MANUSCRIPT

3.6. The genome architectural context of inflammation-induced pri-miR-155 expression

Mapping of the pri-miR-155-associated, LPS-responsive enhancers revealed that these enhancers are located far away (between -54 and -116 Kb) from the TSS of pri-miR-155 gene. Therefore, we wanted to get some insight into whether these enhancers come in close spatial proximity to the TSS of pri-miR-155 gene upon inflammatory stimulus. To identify the basal and inflammation-induced chromatin interactions, we carried out 3C-seq using bait in the region of the most upstream LPS-activated enhancer located_-116 Kb from the miRNA gene in the predicted sub-TAD. We observed both constitutive and LPS-triggered interactions within the predicted sub-TAD of pri-miR-155 (Figure 6). Interestingly, permanent interaction was observed between the -116Kb enhancer and the TSS of pri-miR-155 (Figure 6; red arrow). In addition, LPS-induced interactions were detected between pri-miR-155_-116 Kb and other inflammation responsive enhancers within the sub-TAD (Figure 6; blue arrows).

Collectively, our findings suggest that (i) the identified inflammation responsive enhancers interact with each other and the TSS of pri-miR-155; (ii) the structure of pri-miR-155-associated sub-TAD undergoes inflammation-induced spatial reorganization in macrophages.

4. Discussion

Global miRNA expression analyses and functional studies have revealed important regulatory roles for inflammation responsive miRNAs in macrophage biology such as regulating the defense against infectious agents as well as modulating the initiation and resolution of inflammation (reviewed in [76] and [77]). Nevertheless, genome-wide analysis of the inflammation-modulated mature miRNome does not provide sufficiently detailed insights into the transcriptional and post-transcriptional background of miRNA expression changes. Our work is demonstrating the power and utility of combining genome-wide next generation sequencing technologies to characterize the transcriptional regulation of inflammation responsive miRNAs in LPS-exposed mouse macrophages though the difference in LPS concentrations (10 and 100 ng/ml) between the applied publicly available datasets may be a potential limitation in this study (Figure 7A).

Based on GRO-seq and H3K4m3-specific ChIP-seq datasets, 518 nascent RNA transcripts were detected overlapping with 568 miRNA genes in mouse macrophages. 470 out of 568 of transcribed pri-miRNAs were linked with previously identified TSSs in the integrated miRNA expression and promoter atlas of FANTOM5 database (Supplementary Table 6) [78]. Using our approach, 78% (367/470) of H3K4m3 positive TSSs were localized within +/-1000 bp compared to the FANTOM5 database-derived TSSs confirming the high accuracy of our method, but the distance between the predicted and the previously identified TSSs was higher than 10 Kb in case of 60 miRNA genes including the LPS-repressed miR-30c-1 suggesting the existence of macrophage-specific TSSs/promoters of these miRNA genes (Supplementary Table 6). In addition, we identified the TSSs of 98 miRNA genes which were unidentified previously including the LPS-regulated miR-146a and miR-221/miR-222 polycistron

ACCEPTED MANUSCRIPT

(Supplementary Table 6) completing the collection of miRNA-linked TSSs of the FANTOM5 database [78].

Using a strict statistical test during the small RNA-seq analysis ($p<0.05$, FDR<0.1), 15 LPS responsive mature miRNAs were identified which are regulated at the nascent RNA level in mouse macrophages based on the GRO-seq dataset including the well- established inflammation-associated miR-155, miR-146, miR-221 and miR-125a [41-45, 79, 80]. Interestingly, using a less strict statistical analysis ($p<0.05$ without FDR cut off) has led to the identification of additional 6 miRNAs which are modulated in a similar manner at mature and pri-miRNA levels in independent RNA-seq and GRO-seq datasets suggesting their LPS-dependent regulation (Supplementary Table 5, indicated by red double crosses). Among these miRNAs, we found novel LPS-induced miRNAs such as miR-5107, miR-674 and miR-7043. Interestingly, it has been shown previously that the Th2-type cytokine IL-4 induces miR-5107 expression in a STAT6 independent manner in mouse BMDMs [16]. In addition, miR-5107 expression is influenced in mouse liver and lung following *Schistosoma japonicum* infection suggesting its complex regulation during Th1 and Th2-type immune responses [81].

RNAPII plays a central role in the transcription of miRNAs, but some RNAPIII-transcribed miRNAs have also been identified [7, 8, 23]. We found that all inflammation responsive intergenic and intragenic miRNAs were associated with RNAPII-occupied promoters and enhancers. In addition, RNAPII binding was regulated by LPS and correlated with the presence of active histone mark H3K27Ac and nascent RNA (pri-miRNA and eRNA) expression. Thus, our data suggest that dominantly RNAPII mediates transcription of inflammation responsive miRNAs.

It has recently been described that several transcription factors frequently colocalize and cooperate in so-called hotspot regions of the genome independently from their known binding motifs, and thereby mediate transcriptional programming [82, 83]. LPS-activated TLR4 receptor can activate both NFkB and AP-1 transcription factor complexes leading to the dramatic reprogramming of macrophage transcriptome [74, 84]. Both transcription factor complexes are essential for the inflammation-induced chromosome structure reorganization and DNA loop formation in different myeloid cells [85-87]. We identified two LPS-activated pri-miRNA-associated enhancer subsets based on NFkB-p65 subunit binding including p65-bound ($p65^{high}$) and p65-unbound ($p65^{low}$) enhancers. Interestingly, higher basal and LPS-induced JunB occupancy was observed at p65-bound enhancers compared to p65-unbound enhancers. In addition, the identified binding motifs of these transcriptional factor complexes showed differences between $p65^{high}$ and $p65^{low}$ enhancers. Both NFkB-p65 and Jun-AP1 motifs showed higher enrichment at $p65^{high}$ enhancers compared to the $p65^{low}$ enhancers though Jun-AP1 motif number was more than 3 times higher at both $p65^{high}$ and $p65^{low}$ enhancer sets compared to the NFkB-p65 motif. Finally, while both enhancer subsets proved to be LPS inducible, $p65^{high}$ genomic regions were associated with elevated LPS-induced enhancer activities compared to the $p65^{low}$ enhancers. These data raise the possibility that (i) NFkB-p65 is able to bind non-canonical motifs and/or NFkB and AP-1 complexes may closely collaborate at certain inflammation-activated distal regulatory regions enhancing NFkB-p65 binding and enhancer activity. Nevertheless, further studies are needed to explore the molecular basis of the NFkB-p65 binding and the crosstalk between these transcription factor complexes at the level of individual enhancers.

Repression of nascent RNA expression and enhancer activity triggered by inflammatory signaling pathways has been previously described in macrophages and adipocytes, though the molecular background of inflammation-mediated repression is not completely understood [65, 88, 89]. Two potential mechanisms of inflammation-induced transcriptional repression

ACCEPTED MANUSCRIPT

have been described including (i) TNFα-activated NFkB-directed redistribution of coactivators without direct p65 binding at the repressed enhancers in human adipocytes and (ii) formation of NFkB-p50, NCoR and HDAC3-containing repressosome at the promoter regions of tolerogenic inflammatory genes in LPS-stimulated mouse macrophages [89, 90]. Along with 12 transcriptionally induced miRNAs, we identified 3 transcriptionally repressed miRNAs in LPS-exposed macrophages. These miRNAs were associated with 11 LPS-repressed enhancers, which were localized within the same CTCF/RAD21-established sub-TADs. We observed that the LPS-mediated repression was associated with low NFkB-p65 and JunB occupancies at the enhancers associated with these pri-miRNAs, in agreement with previous studies [65]. Thus, our findings suggest that LPS-induced repression of enhancers associated with repressed pri-miRNAs is likely to be mediated independently of NFkB-p65 and JunB transcription factors. Nevertheless, the exact transcriptional mechanisms by which these pri-miRNAs are repressed remain to be determined.

One of the well-studied inflammatory miRNAs, mir-155, has a conserved immunomodulatory role in many cell types in response to inflammatory signals by limiting the pro-inflammatory gene expression program [41-44, 91]. It has been described that pri-miR-155 expression is induced via the activation of TLR and NOD-like receptor pathways [43, 92]. In addition, LPS-induced pri-miR-155 expression is inhibited by the anti-inflammatory cytokine IL-10 in a STAT3-dependent manner [93]. Here, we aimed to investigate the specific mechanism responsible for the LPS-dependent transcriptional activation of pri-miR-155 expression in macrophages. By combining GRO-seq and H3K4m1 ChIP-seq data, we identified 11 LPS-activated enhancers associated with the miR-155 gene, which clustered into enhancer clusters (super-enhancers). Interestingly, a similar enhancer cluster was observed in TNFα-stimulated human HUVEC cells [94]. Finally, our 3C-seq-based analysis showed the LPS-induced reorganization of the miR-155 gene and formation of interactions between the activated enhancer clusters, the sub-TAD border and the TSS of pri-miR-155. These findings suggest that transcriptional induction of miR-155 expression following inflammatory stimuli involves the activation of miR-155-associated enhancers and the extensive rearrangement of chromosome architecture around the pri-miR-155 gene (Figure 7B).

5. Conclusions

The aim of this study was to investigate the transcriptional basis of inflammation-regulated macrophage miRNome by combining next generation sequencing-based technologies including small RNA-seq, GRO-seq, ChIP-seq, ATAC-seq and 3C-seq. Our next generation sequencing-based approach uncovered the LPS-responsive pri-miRNA and mature miRNA signature in mouse macrophages, and revealed that the majority of LPS-responsive miRNAs are regulated through their transcription and not their maturation. In addition, we show that inflammation-responsive pri-miRNAs are associated with an LPS-sensitive enhancer network. We could distinguish two subsets of inflammation-activated enhancers that showed different NFkB-p65 and JunB binding characteristics and LPS responsiveness. Finally, we demonstrated the LPS-induced reorganization of the pri-miR-155-associated functional chromatin domain. These results are consistent with the notion that transcriptional regulatory mechanisms including modulation of enhancer activity and rearrangement of chromatin structure play an essential role in the control of inflammation-responsive miRNA expression in macrophages. We propose that the complex genomics-bioinformatics approach presented

ACCEPTED MANUSCRIPT

here is amenable to other cell types and other signaling pathways as well, providing a useful tool for the scientific community.

List of abbreviations

miRNAs, microRNAs; RISC, RNA-induced silencing complex; pri-miRNA, primary microRNA; next-generation sequencing, NGS; GRO-seq, Global Run On and sequencing; ChIP-seq, Chromatin Immunoprecpitation and sequencing; small RNA-seq, small RNA sequencing, ATAC-seq, Assay for Transposase-Accessible Chromatin with sequencing; 3C-seq, Chromosome conformation capture sequencing; RNA Polymerase II, RNAPII; IFNγ, interferon gamma; LPS, lipopolysaccharide, IL-4, interleukin-4; JAK, Janus kinase; STAT1, signal transducer and activator of transcription; AP-1, activator protein 1; NFκB , nuclear factor kappa-light-chain-enhancer of activated B cells; BMDM, bone marrow-derived macrophages; qPCR, quantitative PCR

Acknowledgements

The authors would like to acknowledge the technical assistance of Ms. Tímea Cseh, Ms. Beáta Szalka, Ms. Agnes Kriston and the comments on the manuscript by Dr. Beáta Scholtz and members of the Nagy laboratory. L.N. is supported by grants from the Hungarian Scientific Research Fund (OTKA K100196, K111941 and K116855) and by Sanford Burnham Prebys Medical Research Institute. Library preparation and bioinformatics analysis was performed at the Genomic Medicine and Bioinformatic Core Facility of the University of Debrecen. B.D. is supported by an American Heart Association (AHA) postdoctoral fellowship (17POST33660450).

ACCEPTED MANUSCRIPT

Figure legends

Figure 1. LPS-dependent regulation of miRNA expression at the transcriptional level in mouse BMDMs. (A) Heat map showing fold changes of transcriptionally regulated miRNA expression at mature (left panel) and pri-miRNA (right panel) levels in LPS-stimulated macrophages compared with unstimulated control. (B) Genome browser view of GRO-seq data showing the primary RNA transcripts of selected LPS-regulated miRNAs in unstimulated and LPS-stimulated mouse macrophages. Macrophages were treated with LPS for 20, 60 and 180 minutes. (C) RT-qPCR-based validation of pri-miRNA expression in LPS-stimulated and unstimulated macrophages. Macrophages were treated with LPS for 20 minutes as well as 1, 3, 6, 12 and 24 hours. Each data point represents the mean and SD of three biological replicates. **P*<0.05, ***P*<0.01, ****P*<0.001 compared with the unstimulated control marked as 0. (D) Strand-specific GRO-Seq, H3K4m3, H3K27Ac and RNA Pol II-specific ChIP-seq signals in LPS-stimulated and unstimulated mouse macrophages at TSSs and gene bodies of the selected inflammation responsive pri-miRNAs visualized by the Integrative Genomics Viewer.

Figure 2. Identification of LPS-regulated enhancers associated with inflammation responsive miRNA genes in mouse BMDMs with the combination of GRO-seq and H3K4m1-specific ChIP-seq datasets. (A) Box plot representation of H3K4m1 at the activated and repressed pri-miRNA-associated enhancers in LPS-stimulated and unstimulated mouse BMDMs. Macrophages were treated with LPS for 4 hours. (B) Box plot representation of eRNA expression at the activated and repressed pri-miRNA-associated enhancers in LPS-stimulated and unstimulated mouse BMDMs. . Macrophages were treated with LPS for 20, 60 and 180 minutes. (C) Strand-specific GRO-Seq, H3K4m1, CTCF and Rad21-specific ChIP-seq signals in LPS-stimulated and unstimulated mouse macrophages at the genomic loci of miR-155, miR-147 and miR-223 are visualized by the Integrative Genomics Viewer. (D) RT-qPCR-based measurement of eRNA expression of 2-2 selected miR-155, miR-147 and miR-223-associated enhancers in LPS-stimulated and unstimulated macrophages. Macrophages were treated with LPS for 20 minutes as well as 1, 3, 6, 12 and 24 hours. Each data point represents the mean and SD of three biological replicates. **P*<0.05, ***P*<0.01, ****P*<0.001 compared with the unstimulated control marked as 0.

Figure 3. NFkB binding-based characterization of LPS-activated pri-miRNA-associated enhancers. (A) The ratio of NFkB subunit p65-bound ($p65^{high}$) and un-bound ($p65^{low}$) LPS-activated and repressed pri-miRNA-associated enhancers in mouse BMDMs. (B) Box plot representation of NFkB-p65 binding at $p65^{high}$ and $p65^{low}$ LPS-activated as well as LPS-repressed enhancers in LPS-stimulated and unstimulated (ctrl) mouse macrophages. Macrophages were treated with LPS for 3 hours. (C) Box plot representation of JunB binding at $p65^{high}$ and $p65^{low}$ LPS-activated as well as LPS-repressed enhancers in LPS-stimulated and unstimulated mouse macrophages. Macrophages were treated with LPS for 4 hours. (D) Targeted NFkB-p65 and Jun-AP1 binding motif identification at $p65^{high}$ and $p65^{low}$ LPS-activated as well as LPS-repressed enhancers (identified motif number/motif ″positive″ enhancers).

ACCEPTED MANUSCRIPT

Figure 4. Characterization of p65^{high} and p65^{low} pri-miRNA-associated enhancers in mouse BMDMs. (A) Box plot representation of the ATAC-seq intensities at p65^{high} and p65^{low} LPS-activated as well as LPS-repressed enhancers in unstimulated and LPS-stimulated macrophages. Macrophages were treated with LPS for 2 and 6 hours. (B) Box plot representation of H3K4m1 enrichment at p65^{high} and p65^{low} LPS-activated enhancers in LPS-stimulated and unstimulated mouse macrophages. Macrophages were treated with LPS for 4 hours. (C) Box plot representation of H3K27Ac enrichment at p65^{high} and p65^{low} LPS-activated as well as LPS-repressed enhancers in unstimulated and LPS-stimulated macrophages. Macrophages were treated with LPS for 4 hours. (D) Box plot representation of RNA Pol II binding at p65^{high} and p65^{low} LPS-activated as well as LPS-repressed enhancers in unstimulated and LPS-stimulated macrophages. Macrophages were treated with LPS for 4 hours. (E) Strand-specific GRO-Seq, H3K4m1, H3K27Ac, NFkB-p65, JunB and RNAPII ChIP-Seq signals at the selected p65^{high} and p65^{low} LPS-activated as well as LPS-repressed enhancers in LPS-stimulated and unstimulated mouse macrophages. GRO-seq as well as ChIP-seq for the indicated factors and post-translational histone modifications are visualized by the Integrative Genomics Viewer.

Figure 5. Functional characterization of selected pri-miR-155 and pri-miR-147-associated LPS-activated p65^{high} and p65^{low} enhancers in mouse inflammatory macrophages. ChIP-qPCR measurements against RNA Pol II-pS5, RNA Pol II-pS2, Pu.1, NFkB-p65 and p300 on selected LPS-activated enhancers and negative control Prmt8 enhancer (Prmt8e) regions from wild-type unstimulated and LPS- stimulated macrophages. Macrophages were treated with LPS for 1, 6 and 24 hours. The mean and ±SD of two biological replicates are shown. *P<0.05, **P<0.01, ***P<0.001 compared with the unstimulated control marked as 0.

Figure 6. Basal and inflammation-induced chromatin interactions between the LPS-activated enhancers and the TSS of pri-miR155 within the miR-155-associated sub-TAD. Genome browser view of the *pri-miR-155* locus containing proximal interacting regions of the intergenic bait in LPS-stimulated and unstimulated mouse BMDMs as well as loop predictions generated based on CTCF/RAD21-cobound regions. Asterisks show the site of the specific bait. GRO-seq and ChIP-seq for the indicated factors are shown. Green arrowheads and gray dashed lines indicate the predicted domain borders.

Figure 7. Schematic representation of the experimental pipeline and proposed regulation of miR-155. (A) Flowchart showing genomics and bioinformatics pipeline utilized in the characterization of transcriptionally-regulated LPS-responsive miRNAs in mouse macrophages. (B) Schematic representation of LPS-induced pri-miR-155 transcription in mouse macrophages.

ACCEPTED MANUSCRIPT

References

[1] M. Ghildiyal, P.D. Zamore, Small silencing RNAs: an expanding universe, Nature reviews. Genetics, 10 (2009) 94-108.
[2] D.P. Bartel, MicroRNAs: genomics, biogenesis, mechanism, and function, Cell, 116 (2004) 281-297.
[3] G. Stefani, F.J. Slack, Small non-coding RNAs in animal development, Nature reviews. Molecular cell biology, 9 (2008) 219-230.
[4] K.N. Ivey, D. Srivastava, MicroRNAs as regulators of differentiation and cell fate decisions, Cell stem cell, 7 (2010) 36-41.
[5] L. Du, A. Pertsemlidis, Cancer and neurodegenerative disorders: pathogenic convergence through microRNA regulation, Journal of molecular cell biology, 3 (2011) 176-180.
[6] D.P. Bartel, C.Z. Chen, Micromanagers of gene expression: the potentially widespread influence of metazoan microRNAs, Nature reviews. Genetics, 5 (2004) 396-400.
[7] Y. Lee, M. Kim, J. Han, K.H. Yeom, S. Lee, S.H. Baek, V.N. Kim, MicroRNA genes are transcribed by RNA polymerase II, The EMBO journal, 23 (2004) 4051-4060.
[8] G.M. Borchert, W. Lanier, B.L. Davidson, RNA polymerase III transcribes human microRNAs, Nature structural & molecular biology, 13 (2006) 1097-1101.
[9] B.M. Engels, G. Hutvagner, Principles and effects of microRNA-mediated post-transcriptional gene regulation, Oncogene, 25 (2006) 6163-6169.
[10] E. Huntzinger, E. Izaurralde, Gene silencing by microRNAs: contributions of translational repression and mRNA decay, Nature reviews. Genetics, 12 (2011) 99-110.
[11] M. Ha, V.N. Kim, Regulation of microRNA biogenesis, Nature reviews. Molecular cell biology, 15 (2014) 509-524.
[12] P.K. Rao, R.M. Kumar, M. Farkhondeh, S. Baskerville, H.F. Lodish, Myogenic factors that regulate expression of muscle-specific microRNAs, Proceedings of the National Academy of Sciences of the United States of America, 103 (2006) 8721-8726.
[13] T.C. Chang, D. Yu, Y.S. Lee, E.A. Wentzel, D.E. Arking, K.M. West, C.V. Dang, A. Thomas-Tikhonenko, J.T. Mendell, Widespread microRNA repression by Myc contributes to tumorigenesis, Nature genetics, 40 (2008) 43-50.
[14] N. Liu, A.H. Williams, Y. Kim, J. McAnally, S. Bezprozvannaya, L.B. Sutherland, J.A. Richardson, R. Bassel-Duby, E.N. Olson, An intragenic MEF2-dependent enhancer directs muscle-specific expression of microRNAs 1 and 133, Proceedings of the National Academy of Sciences of the United States of America, 104 (2007) 20844-20849.
[15] K. Woods, J.M. Thomson, S.M. Hammond, Direct regulation of an oncogenic micro-RNA cluster by E2F transcription factors, The Journal of biological chemistry, 282 (2007) 2130-2134.
[16] Z. Czimmerer, T. Varga, M. Kiss, C.O. Vazquez, Q.M. Doan-Xuan, D. Ruckerl, S.G. Tattikota, X. Yan, Z.S. Nagy, B. Daniel, S. Poliska, A. Horvath, G. Nagy, E. Varallyay, M.N. Poy, J.E. Allen, Z. Bacso, C. Abreu-Goodger, L. Nagy, The IL-4/STAT6 signaling axis establishes a conserved microRNA signature in human and mouse macrophages regulating cell survival via miR-342-3p, Genome medicine, 8 (2016) 63.
[17] H.K. Saini, S. Griffiths-Jones, A.J. Enright, Genomic analysis of human microRNA transcripts, Proceedings of the National Academy of Sciences of the United States of America, 104 (2007) 17719-17724.
[18] N. Hah, C.G. Danko, L. Core, J.J. Waterfall, A. Siepel, J.T. Lis, W.L. Kraus, A rapid, extensive, and transient transcriptional response to estrogen signaling in breast cancer cells, Cell, 145 (2011) 622-634.
[19] C. Nepal, M. Coolen, Y. Hadzhiev, D. Cussigh, P. Mydel, V.M. Steen, P. Carninci, J.B. Andersen, L. Bally-Cuif, F. Muller, B. Lenhard, Transcriptional, post-transcriptional and chromatin-associated regulation of pri-miRNAs, pre-miRNAs and moRNAs, Nucleic acids research, 44 (2016) 3070-3081.

ACCEPTED MANUSCRIPT

[20] S. Mei, Y. Liu, Y. Bao, Y. Zhang, S. Min, Y. Liu, Y. Huang, X. Yuan, Y. Feng, J. Shi, R. Yang, Dendritic cell-associated miRNAs are modulated via chromatin remodeling in response to different environments, PloS one, 9 (2014) e90231.
[21] H. Suzuki, S. Takatsuka, H. Akashi, E. Yamamoto, M. Nojima, R. Maruyama, M. Kai, H.O. Yamano, Y. Sasaki, T. Tokino, Y. Shinomura, K. Imai, M. Toyota, Genome-wide profiling of chromatin signatures reveals epigenetic regulation of MicroRNA genes in colorectal cancer, Cancer research, 71 (2011) 5646-5658.
[22] M. Chae, C.G. Danko, W.L. Kraus, groHMM: a computational tool for identifying unannotated and cell type-specific transcription units from global run-on sequencing data, BMC bioinformatics, 16 (2015) 222.
[23] F. Ozsolak, L.L. Poling, Z. Wang, H. Liu, X.S. Liu, R.G. Roeder, X. Zhang, J.S. Song, D.E. Fisher, Chromatin structure analyses identify miRNA promoters, Genes & development, 22 (2008) 3172-3183.
[24] C.H. Chien, Y.M. Sun, W.C. Chang, P.Y. Chiang-Hsieh, T.Y. Lee, W.C. Tsai, J.T. Horng, A.P. Tsou, H.D. Huang, Identifying transcriptional start sites of human microRNAs based on high-throughput sequencing data, Nucleic acids research, 39 (2011) 9345-9356.
[25] M. Bulger, M. Groudine, Functional and mechanistic diversity of distal transcription enhancers, Cell, 144 (2011) 327-339.
[26] D. Shlyueva, G. Stampfel, A. Stark, Transcriptional enhancers: from properties to genome-wide predictions, Nature reviews. Genetics, 15 (2014) 272-286.
[27] C.T. Ong, V.G. Corces, Enhancer function: new insights into the regulation of tissue-specific gene expression, Nature reviews. Genetics, 12 (2011) 283-293.
[28] D. Chen, L.Y. Fu, Z. Zhang, G. Li, H. Zhang, L. Jiang, A.P. Harrison, H.P. Shanahan, C. Klukas, H.Y. Zhang, Y. Ruan, L.L. Chen, M. Chen, Dissecting the chromatin interactome of microRNA genes, Nucleic acids research, 42 (2014) 3028-3043.
[29] J.H. Cheng, D.Z. Pan, Z.T. Tsai, H.K. Tsai, Genome-wide analysis of enhancer RNA in gene regulation across 12 mouse tissues, Scientific reports, 5 (2015) 12648.
[30] S. Gordon, P.R. Taylor, Monocyte and macrophage heterogeneity, Nature reviews. Immunology, 5 (2005) 953-964.
[31] D.M. Mosser, J.P. Edwards, Exploring the full spectrum of macrophage activation, Nature reviews. Immunology, 8 (2008) 958-969.
[32] A. Mantovani, A. Sica, S. Sozzani, P. Allavena, A. Vecchi, M. Locati, The chemokine system in diverse forms of macrophage activation and polarization, Trends in immunology, 25 (2004) 677-686.
[33] T. Lawrence, G. Natoli, Transcriptional regulation of macrophage polarization: enabling diversity with identity, Nature reviews. Immunology, 11 (2011) 750-761.
[34] A. Androulidaki, D. Iliopoulos, A. Arranz, C. Doxaki, S. Schworer, V. Zacharioudaki, A.N. Margioris, P.N. Tsichlis, C. Tsatsanis, The kinase Akt1 controls macrophage response to lipopolysaccharide by regulating microRNAs, Immunity, 31 (2009) 220-231.
[35] N. Xie, H. Cui, S. Banerjee, Z. Tan, R. Salomao, M. Fu, E. Abraham, V.J. Thannickal, G. Liu, miR-27a regulates inflammatory response of macrophages by targeting IL-10, Journal of immunology, 193 (2014) 327-334.
[36] C.E. Monk, G. Hutvagner, J.S. Arthur, Regulation of miRNA transcription in macrophages in response to Candida albicans, PloS one, 5 (2010) e13669.
[37] M. Nazari-Jahantigh, Y. Wei, H. Noels, S. Akhtar, Z. Zhou, R.R. Koenen, K. Heyll, F. Gremse, F. Kiessling, J. Grommes, C. Weber, A. Schober, MicroRNA-155 promotes atherosclerosis by repressing Bcl6 in macrophages, The Journal of clinical investigation, 122 (2012) 4190-4202.
[38] G. Liu, A. Friggeri, Y. Yang, Y.J. Park, Y. Tsuruta, E. Abraham, miR-147, a microRNA that is induced upon Toll-like receptor stimulation, regulates murine macrophage inflammatory responses, Proceedings of the National Academy of Sciences of the United States of America, 106 (2009) 15819-15824.

ACCEPTED MANUSCRIPT

[39] Q. Chen, H. Wang, Y. Liu, Y. Song, L. Lai, Q. Han, X. Cao, Q. Wang, Inducible microRNA-223 down-regulation promotes TLR-triggered IL-6 and IL-1beta production in macrophages by targeting STAT3, PloS one, 7 (2012) e42971.
[40] J. Wang, X. Bai, Q. Song, F. Fan, Z. Hu, G. Cheng, Y. Zhang, miR-223 Inhibits Lipid Deposition and Inflammation by Suppressing Toll-Like Receptor 4 Signaling in Macrophages, International journal of molecular sciences, 16 (2015) 24965-24982.
[41] E. Tili, J.J. Michaille, A. Cimino, S. Costinean, C.D. Dumitru, B. Adair, M. Fabbri, H. Alder, C.G. Liu, G.A. Calin, C.M. Croce, Modulation of miR-155 and miR-125b levels following lipopolysaccharide/TNF-alpha stimulation and their possible roles in regulating the response to endotoxin shock, Journal of immunology, 179 (2007) 5082-5089.
[42] R.M. O'Connell, A.A. Chaudhuri, D.S. Rao, D. Baltimore, Inositol phosphatase SHIP1 is a primary target of miR-155, Proceedings of the National Academy of Sciences of the United States of America, 106 (2009) 7113-7118.
[43] L.N. Schulte, A.J. Westermann, J. Vogel, Differential activation and functional specialization of miR-146 and miR-155 in innate immune sensing, Nucleic acids research, 41 (2013) 542-553.
[44] K.A. Jablonski, A.D. Gaudet, S.A. Amici, P.G. Popovich, M. Guerau-de-Arellano, Control of the Inflammatory Macrophage Transcriptional Signature by miR-155, PloS one, 11 (2016) e0159724.
[45] K.D. Taganov, M.P. Boldin, K.J. Chang, D. Baltimore, NF-kappaB-dependent induction of microRNA miR-146, an inhibitor targeted to signaling proteins of innate immune responses, Proceedings of the National Academy of Sciences of the United States of America, 103 (2006) 12481-12486.
[46] B. Daniel, G. Nagy, N. Hah, A. Horvath, Z. Czimmerer, S. Poliska, T. Gyuris, J. Keirsse, C. Gysemans, J.A. Van Ginderachter, B.L. Balint, R.M. Evans, E. Barta, L. Nagy, The active enhancer network operated by liganded RXR supports angiogenic activity in macrophages, Genes & development, 28 (2014) 1562-1577.
[47] P. Flicek, M.R. Amode, D. Barrell, K. Beal, K. Billis, S. Brent, D. Carvalho-Silva, P. Clapham, G. Coates, S. Fitzgerald, L. Gil, C.G. Giron, L. Gordon, T. Hourlier, S. Hunt, N. Johnson, T. Juettemann, A.K. Kahari, S. Keenan, E. Kulesha, F.J. Martin, T. Maurel, W.M. McLaren, D.N. Murphy, R. Nag, B. Overduin, M. Pignatelli, B. Pritchard, E. Pritchard, H.S. Riat, M. Ruffier, D. Sheppard, K. Taylor, A. Thormann, S.J. Trevanion, A. Vullo, S.P. Wilder, M. Wilson, A. Zadissa, B.L. Aken, E. Birney, F. Cunningham, J. Harrow, J. Herrero, T.J. Hubbard, R. Kinsella, M. Muffato, A. Parker, G. Spudich, A. Yates, D.R. Zerbino, S.M. Searle, Ensembl 2014, Nucleic acids research, 42 (2014) D749-755.
[48] A. Kozomara, S. Griffiths-Jones, miRBase: annotating high confidence microRNAs using deep sequencing data, Nucleic acids research, 42 (2014) D68-73.
[49] E. Barta, Command line analysis of ChIP-seq results, (2011).
[50] H. Li, R. Durbin, Fast and accurate short read alignment with Burrows-Wheeler transform, Bioinformatics, 25 (2009) 1754-1760.
[51] Y. Zhang, T. Liu, C.A. Meyer, J. Eeckhoute, D.S. Johnson, B.E. Bernstein, C. Nusbaum, R.M. Myers, M. Brown, W. Li, X.S. Liu, Model-based analysis of ChIP-Seq (MACS), Genome biology, 9 (2008) R137.
[52] S. Heinz, C. Benner, N. Spann, E. Bertolino, Y.C. Lin, P. Laslo, J.X. Cheng, C. Murre, H. Singh, C.K. Glass, Simple combinations of lineage-determining transcription factors prime cis-regulatory elements required for macrophage and B cell identities, Molecular cell, 38 (2010) 576-589.
[53] E.P. Consortium, An integrated encyclopedia of DNA elements in the human genome, Nature, 489 (2012) 57-74.
[54] C.S. Ross-Innes, R. Stark, A.E. Teschendorff, K.A. Holmes, H.R. Ali, M.J. Dunning, G.D. Brown, O. Gojis, I.O. Ellis, A.R. Green, S. Ali, S.F. Chin, C. Palmieri, C. Caldas, J.S. Carroll, Differential oestrogen receptor binding is associated with clinical outcome in breast cancer, Nature, 481 (2012) 389-393.
[55] A.R. Quinlan, I.M. Hall, BEDTools: a flexible suite of utilities for comparing genomic features, Bioinformatics, 26 (2010) 841-842.
[56] H.A. Kestler, A. Muller, J.M. Kraus, M. Buchholz, T.M. Gress, H. Liu, D.W. Kane, B.R. Zeeberg, J.N. Weinstein, VennMaster: area-proportional Euler diagrams for functional GO analysis of microarrays, BMC bioinformatics, 9 (2008) 67.

ACCEPTED MANUSCRIPT

[57] H. Thorvaldsdottir, J.T. Robinson, J.P. Mesirov, Integrative Genomics Viewer (IGV): high-performance genomics data visualization and exploration, Briefings in bioinformatics, 14 (2013) 178-192.
[58] A.J. Saldanha, Java Treeview--extensible visualization of microarray data, Bioinformatics, 20 (2004) 3246-3248.
[59] A.S. Hinrichs, D. Karolchik, R. Baertsch, G.P. Barber, G. Bejerano, H. Clawson, M. Diekhans, T.S. Furey, R.A. Harte, F. Hsu, J. Hillman-Jackson, R.M. Kuhn, J.S. Pedersen, A. Pohl, B.J. Raney, K.R. Rosenbloom, A. Siepel, K.E. Smith, C.W. Sugnet, A. Sultan-Qurraie, D.J. Thomas, H. Trumbower, R.J. Weber, M. Weirauch, A.S. Zweig, D. Haussler, W.J. Kent, The UCSC Genome Browser Database: update 2006, Nucleic acids research, 34 (2006) D590-598.
[60] S.S. Rao, M.H. Huntley, N.C. Durand, E.K. Stamenova, I.D. Bochkov, J.T. Robinson, A.L. Sanborn, I. Machol, A.D. Omer, E.S. Lander, E.L. Aiden, A 3D map of the human genome at kilobase resolution reveals principles of chromatin looping, Cell, 159 (2014) 1665-1680.
[61] G. Nagy, E. Czipa, L. Steiner, T. Nagy, S. Pongor, L. Nagy, E. Barta, Motif oriented high-resolution analysis of ChIP-seq data reveals the topological order of CTCF and cohesin proteins on DNA, BMC genomics, 17 (2016) 637.
[62] B. Daniel, B.L. Balint, Z.S. Nagy, L. Nagy, Mapping the genomic binding sites of the activated retinoid X receptor in murine bone marrow-derived macrophages using chromatin immunoprecipitation sequencing, Methods in molecular biology, 1204 (2014) 15-24.
[63] U.M. Thongjuea S, Medicine WIoM, Oxford Uo and UK, r3Cseq: Analysis of Chromosome Conformation Capture and Next-generation Sequencing (3C-seq). (2016).
[64] R. Ostuni, V. Piccolo, I. Barozzi, S. Polletti, A. Termanini, S. Bonifacio, A. Curina, E. Prosperini, S. Ghisletti, G. Natoli, Latent enhancers activated by stimulation in differentiated cells, Cell, 152 (2013) 157-171.
[65] N. Hah, C. Benner, L.W. Chong, R.T. Yu, M. Downes, R.M. Evans, Inflammation-sensitive super enhancers form domains of coordinately regulated enhancer RNAs, Proceedings of the National Academy of Sciences of the United States of America, 112 (2015) E297-302.
[66] A. Barski, S. Cuddapah, K. Cui, T.Y. Roh, D.E. Schones, Z. Wang, G. Wei, I. Chepelev, K. Zhao, High-resolution profiling of histone methylations in the human genome, Cell, 129 (2007) 823-837.
[67] S. Heinz, C.E. Romanoski, C. Benner, C.K. Glass, The selection and function of cell type-specific enhancers, Nature reviews. Molecular cell biology, 16 (2015) 144-154.
[68] G. Natoli, J.C. Andrau, Noncoding transcription at enhancers: general principles and functional models, Annual review of genetics, 46 (2012) 1-19.
[69] V.C. Seitan, A.J. Faure, Y. Zhan, R.P. McCord, B.R. Lajoie, E. Ing-Simmons, B. Lenhard, L. Giorgetti, E. Heard, A.G. Fisher, P. Flicek, J. Dekker, M. Merkenschlager, Cohesin-based chromatin interactions enable regulated gene expression within preexisting architectural compartments, Genome research, 23 (2013) 2066-2077.
[70] S. Sofueva, E. Yaffe, W.C. Chan, D. Georgopoulou, M. Vietri Rudan, H. Mira-Bontenbal, S.M. Pollard, G.P. Schroth, A. Tanay, S. Hadjur, Cohesin-mediated interactions organize chromosomal domain architecture, The EMBO journal, 32 (2013) 3119-3129.
[71] T. Xiao, J. Wallace, G. Felsenfeld, Specific sites in the C terminus of CTCF interact with the SA2 subunit of the cohesin complex and are required for cohesin-dependent insulation activity, Molecular and cellular biology, 31 (2011) 2174-2183.
[72] G.D. Barish, R.T. Yu, M. Karunasiri, C.B. Ocampo, J. Dixon, C. Benner, A.L. Dent, R.K. Tangirala, R.M. Evans, Bcl-6 and NF-kappaB cistromes mediate opposing regulation of the innate immune response, Genes & development, 24 (2010) 2760-2765.
[73] M.U. Kaikkonen, N.J. Spann, S. Heinz, C.E. Romanoski, K.A. Allison, J.D. Stender, H.B. Chun, D.F. Tough, R.K. Prinjha, C. Benner, C.K. Glass, Remodeling of the enhancer landscape during macrophage activation is coupled to enhancer transcription, Molecular cell, 51 (2013) 310-325.
[74] C.K. Glass, G. Natoli, Molecular control of activation and priming in macrophages, Nature immunology, 17 (2016) 26-33.

ACCEPTED MANUSCRIPT

[75] M.K. Atianand, W. Hu, A.T. Satpathy, Y. Shen, E.P. Ricci, J.R. Alvarez-Dominguez, A. Bhatta, S.A. Schattgen, J.D. McGowan, J. Blin, J.E. Braun, P. Gandhi, M.J. Moore, H.Y. Chang, H.F. Lodish, D.R. Caffrey, K.A. Fitzgerald, A Long Noncoding RNA lincRNA-EPS Acts as a Transcriptional Brake to Restrain Inflammation, Cell, 165 (2016) 1672-1685.
[76] Y. Wei, A. Schober, MicroRNA regulation of macrophages in human pathologies, Cellular and molecular life sciences : CMLS, 73 (2016) 3473-3495.
[77] X.Q. Wu, Y. Dai, Y. Yang, C. Huang, X.M. Meng, B.M. Wu, J. Li, Emerging role of microRNAs in regulating macrophage activation and polarization in immune response and inflammation, Immunology, 148 (2016) 237-248.
[78] D. de Rie, I. Abugessaisa, T. Alam, E. Arner, P. Arner, H. Ashoor, G. Astrom, M. Babina, N. Bertin, A.M. Burroughs, A.J. Carlisle, C.O. Daub, M. Detmar, R. Deviatiiarov, A. Fort, C. Gebhard, D. Goldowitz, S. Guhl, T.J. Ha, J. Harshbarger, A. Hasegawa, K. Hashimoto, M. Herlyn, P. Heutink, K.J. Hitchens, C.C. Hon, E. Huang, Y. Ishizu, C. Kai, T. Kasukawa, P. Klinken, T. Lassmann, C.H. Lecellier, W. Lee, M. Lizio, V. Makeev, A. Mathelier, Y.A. Medvedeva, N. Mejhert, C.J. Mungall, S. Noma, M. Ohshima, M. Okada-Hatakeyama, H. Persson, P. Rizzu, F. Roudnicky, P. Saetrom, H. Sato, J. Severin, J.W. Shin, R.K. Swoboda, H. Tarui, H. Toyoda, K. Vitting-Seerup, L. Winteringham, Y. Yamaguchi, K. Yasuzawa, M. Yoneda, N. Yumoto, S. Zabierowski, P.G. Zhang, C.A. Wells, K.M. Summers, H. Kawaji, A. Sandelin, M. Rehli, F. Consortium, Y. Hayashizaki, P. Carninci, A.R.R. Forrest, M.J.L. de Hoon, An integrated expression atlas of miRNAs and their promoters in human and mouse, Nature biotechnology, 35 (2017) 872-878.
[79] M. El Gazzar, C.E. McCall, MicroRNAs distinguish translational from transcriptional silencing during endotoxin tolerance, The Journal of biological chemistry, 285 (2010) 20940-20951.
[80] J.W. Graff, A.M. Dickson, G. Clay, A.P. McCaffrey, M.E. Wilson, Identifying functional microRNAs in macrophages with polarized phenotypes, The Journal of biological chemistry, 287 (2012) 21816-21825.
[81] H. Han, J. Peng, Y. Hong, M. Zhang, Y. Han, D. Liu, Z. Fu, Y. Shi, J. Xu, J. Tao, J. Lin, MicroRNA expression profile in different tissues of BALB/c mice in the early phase of Schistosoma japonicum infection, Molecular and biochemical parasitology, 188 (2013) 1-9.
[82] R. Siersbaek, S. Baek, A. Rabiee, R. Nielsen, S. Traynor, N. Clark, A. Sandelin, O.N. Jensen, M.H. Sung, G.L. Hager, S. Mandrup, Molecular architecture of transcription factor hotspots in early adipogenesis, Cell reports, 7 (2014) 1434-1442.
[83] R. Siersbaek, A. Rabiee, R. Nielsen, S. Sidoli, S. Traynor, A. Loft, L. La Cour Poulsen, A. Rogowska-Wrzesinska, O.N. Jensen, S. Mandrup, Transcription factor cooperativity in early adipogenic hotspots and super-enhancers, Cell reports, 7 (2014) 1443-1455.
[84] T. Kawai, S. Akira, TLR signaling, Cell death and differentiation, 13 (2006) 816-825.
[85] H. Guo, Z. Mi, P.C. Kuo, Characterization of short range DNA looping in endotoxin-mediated transcription of the murine inducible nitric-oxide synthase (iNOS) gene, The Journal of biological chemistry, 283 (2008) 25209-25217.
[86] W. Zhao, L. Wang, M. Zhang, P. Wang, L. Zhang, C. Yuan, J. Qi, Y. Qiao, P.C. Kuo, C. Gao, NF-kappaB- and AP-1-mediated DNA looping regulates osteopontin transcription in endotoxin-stimulated murine macrophages, Journal of immunology, 186 (2011) 3173-3179.
[87] Y.J. Chen, L.S. Chang, NFkappaB- and AP-1-mediated DNA looping regulates matrix metalloproteinase-9 transcription in TNF-alpha-treated human leukemia U937 cells, Biochimica et biophysica acta, 1849 (2015) 1248-1259.
[88] D.M. Bhatt, A. Pandya-Jones, A.J. Tong, I. Barozzi, M.M. Lissner, G. Natoli, D.L. Black, S.T. Smale, Transcript dynamics of proinflammatory genes revealed by sequence analysis of subcellular RNA fractions, Cell, 150 (2012) 279-290.
[89] S.F. Schmidt, B.D. Larsen, A. Loft, R. Nielsen, J.G. Madsen, S. Mandrup, Acute TNF-induced repression of cell identity genes is mediated by NFkappaB-directed redistribution of cofactors from super-enhancers, Genome research, 25 (2015) 1281-1294.
[90] Q. Yan, R.J. Carmody, Z. Qu, Q. Ruan, J. Jager, S.E. Mullican, M.A. Lazar, Y.H. Chen, Nuclear factor-kappaB binding motifs specify Toll-like receptor-induced gene repression through an inducible

ACCEPTED MANUSCRIPT

repressosome, Proceedings of the National Academy of Sciences of the United States of America, 109 (2012) 14140-14145.
[91] M. Ceppi, P.M. Pereira, I. Dunand-Sauthier, E. Barras, W. Reith, M.A. Santos, P. Pierre, MicroRNA-155 modulates the interleukin-1 signaling pathway in activated human monocyte-derived dendritic cells, Proceedings of the National Academy of Sciences of the United States of America, 106 (2009) 2735-2740.
[92] M. Koch, H.J. Mollenkopf, U. Klemm, T.F. Meyer, Induction of microRNA-155 is TLR- and type IV secretion system-dependent in macrophages and inhibits DNA-damage induced apoptosis, Proceedings of the National Academy of Sciences of the United States of America, 109 (2012) E1153-1162.
[93] C.E. McCoy, F.J. Sheedy, J.E. Qualls, S.L. Doyle, S.R. Quinn, P.J. Murray, L.A. O'Neill, IL-10 inhibits miR-155 induction by toll-like receptors, The Journal of biological chemistry, 285 (2010) 20492-20498.
[94] Q. Duan, X. Mao, Y. Xiao, Z. Liu, Y. Wang, H. Zhou, Z. Zhou, J. Cai, K. Xia, Q. Zhu, J. Qi, H. Huang, J. Plutzky, T. Yang, Super enhancers at the miR-146a and miR-155 genes contribute to self-regulation of inflammation, Biochimica et biophysica acta, 1859 (2016) 564-571.

ACCEPTED MANUSCRIPT

ACCEPTED MANUSCRIPT

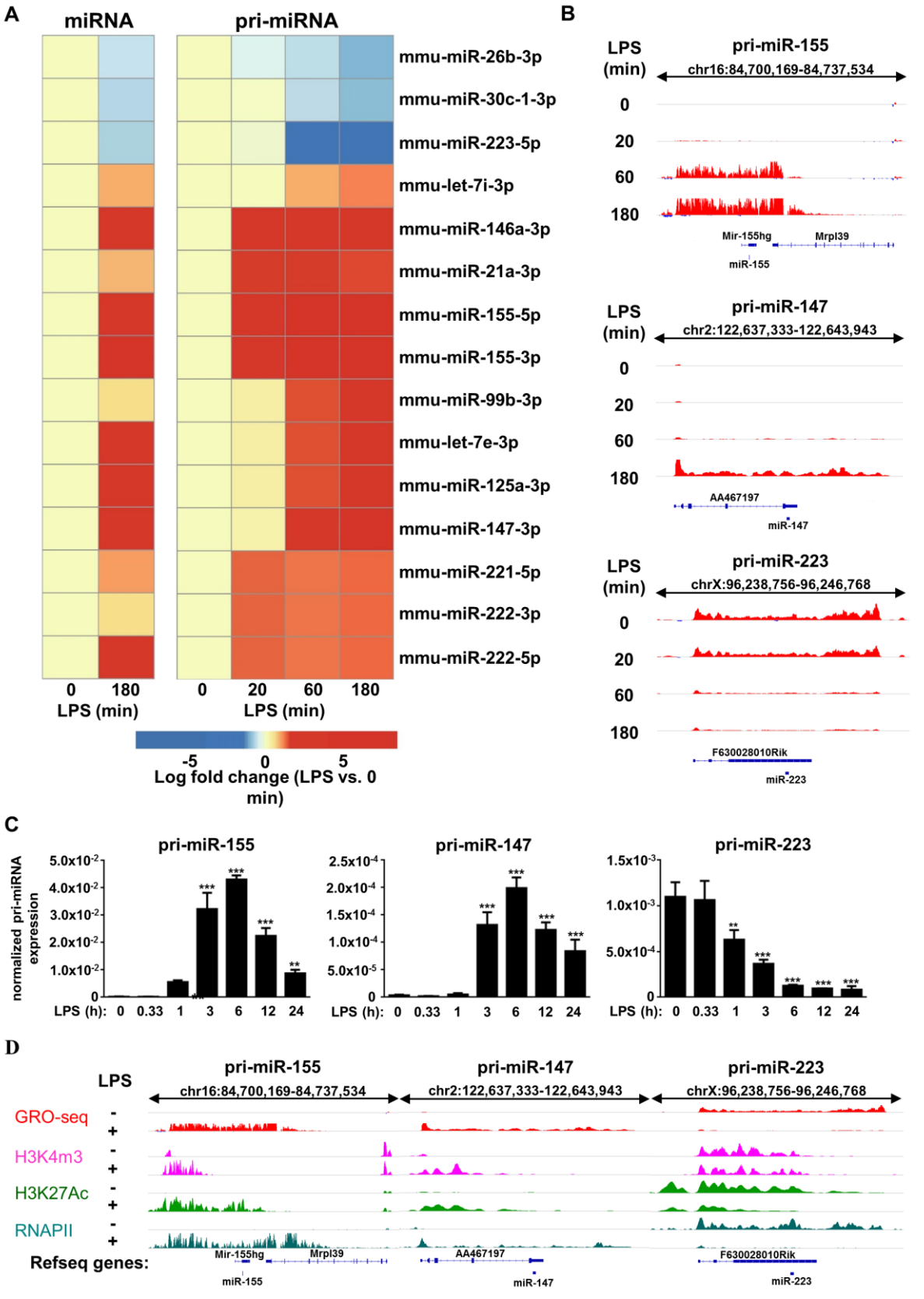

Figure 1

ACCEPTED MANUSCRIPT

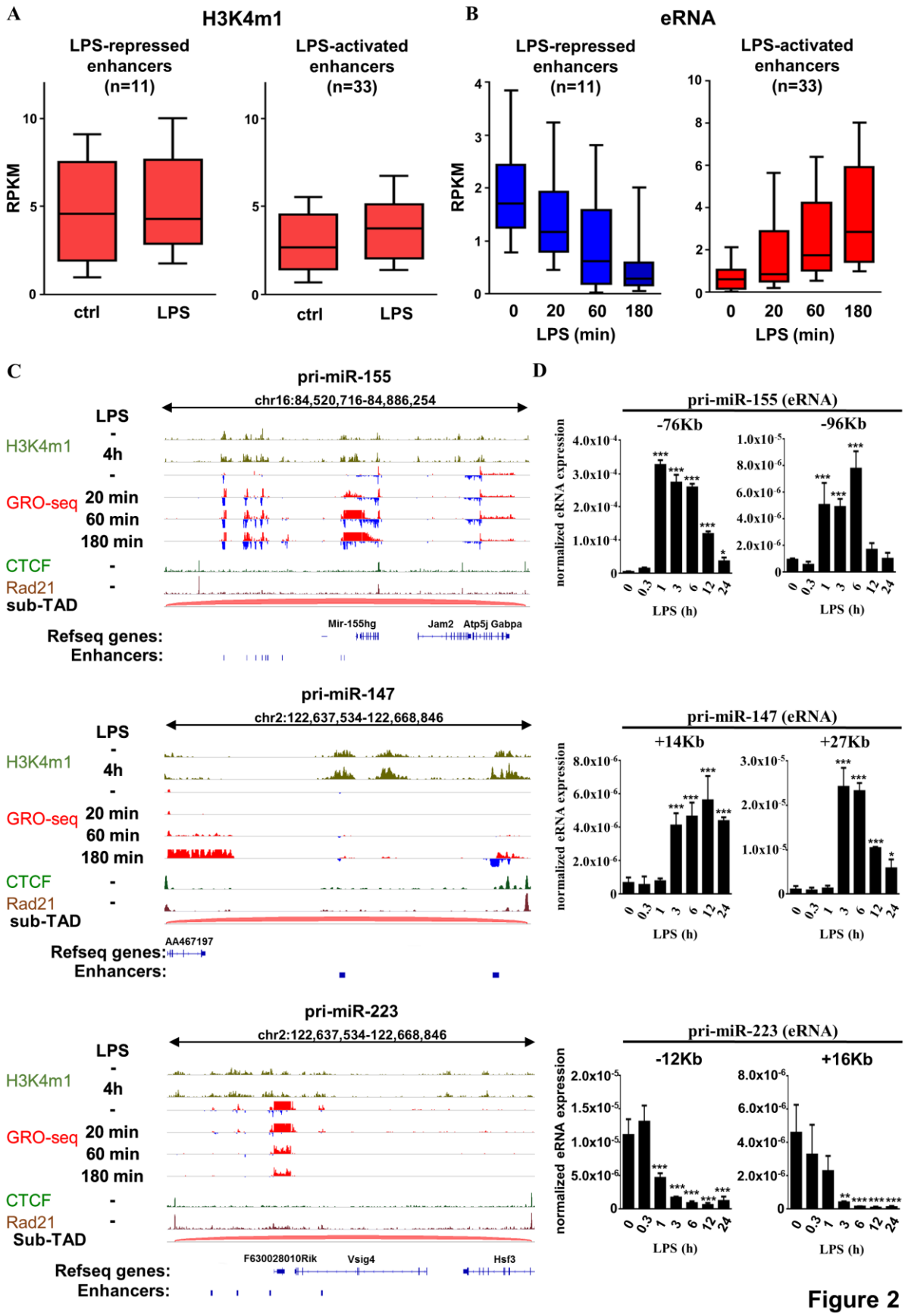

Figure 2

ACCEPTED MANUSCRIPT

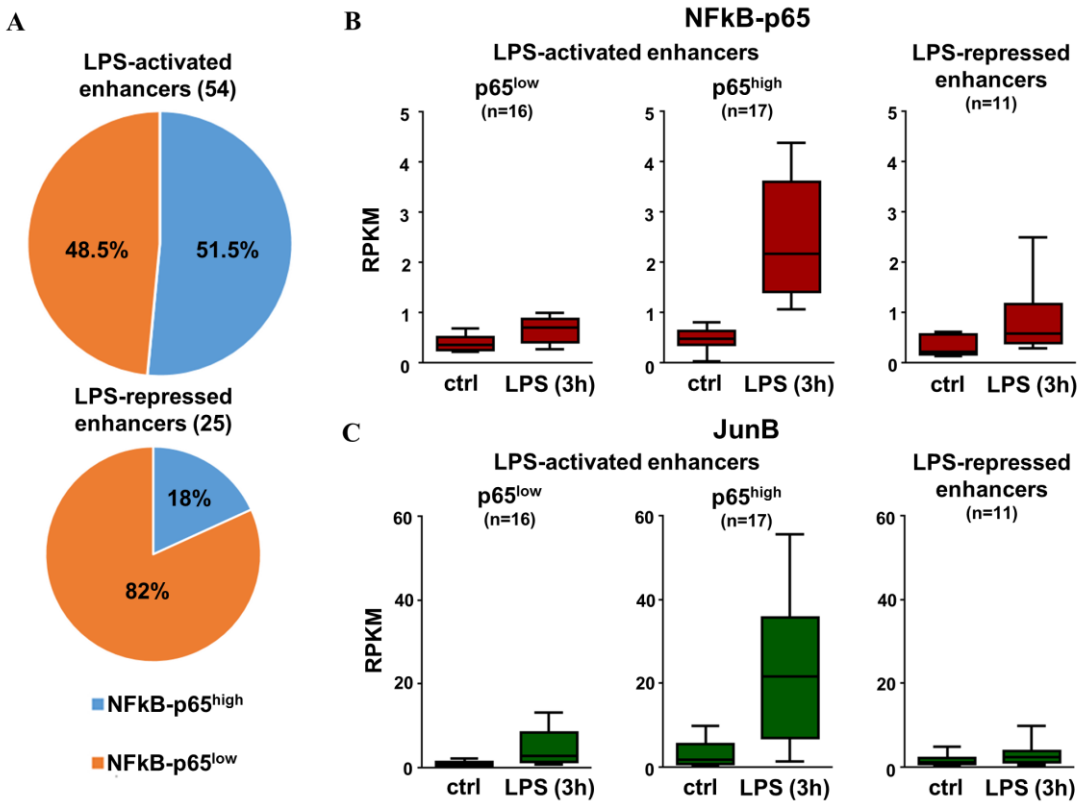

D

	Motif	LPS-activated enhancers p65high	LPS-activated enhancers p65low	LPS-repressed enhancers
NFkB-p65		8/5	5/3	0/0
Jun-AP1		30/12	18/7	6/3

Figure 3

ACCEPTED MANUSCRIPT

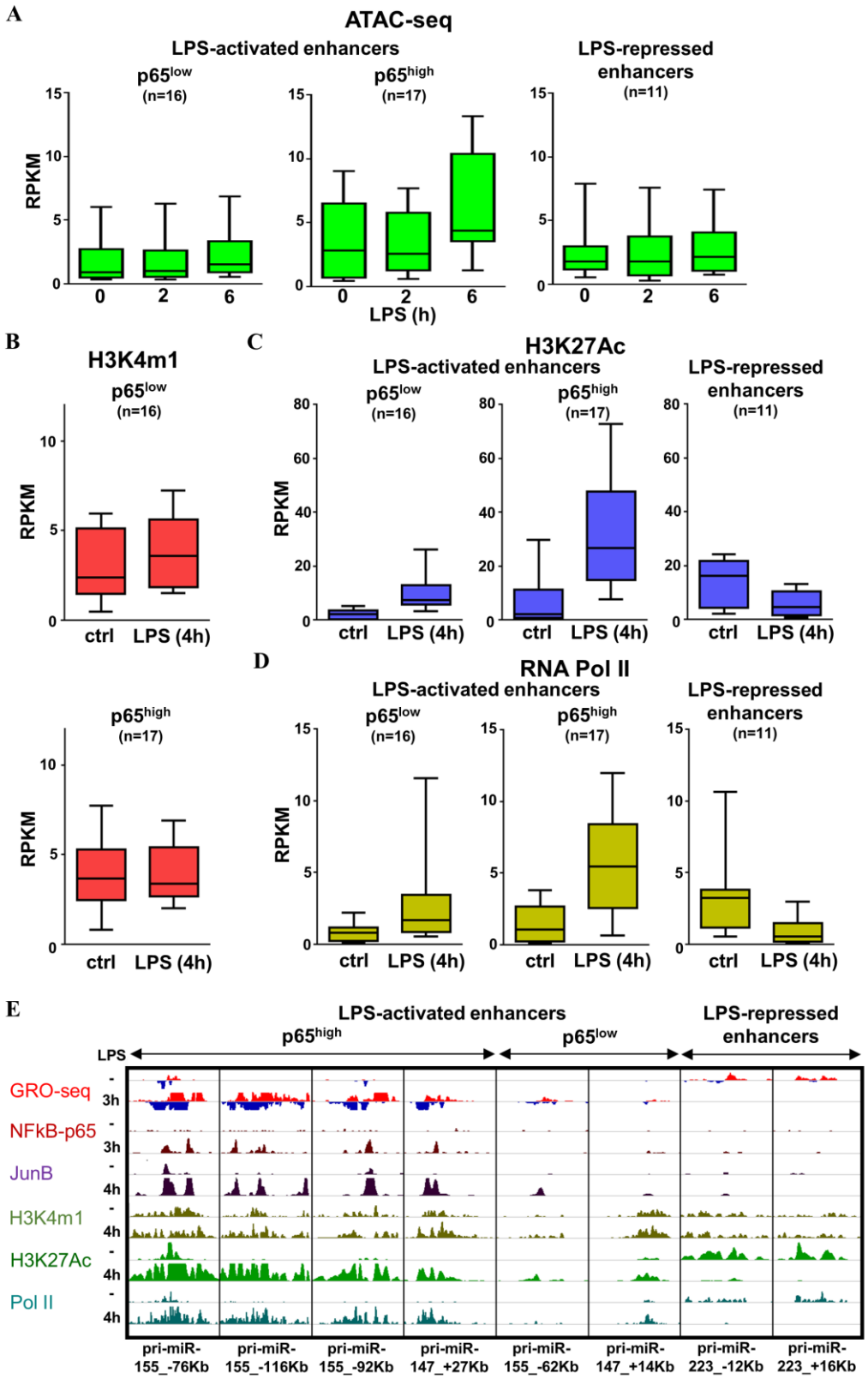

Figure 4

ACCEPTED MANUSCRIPT

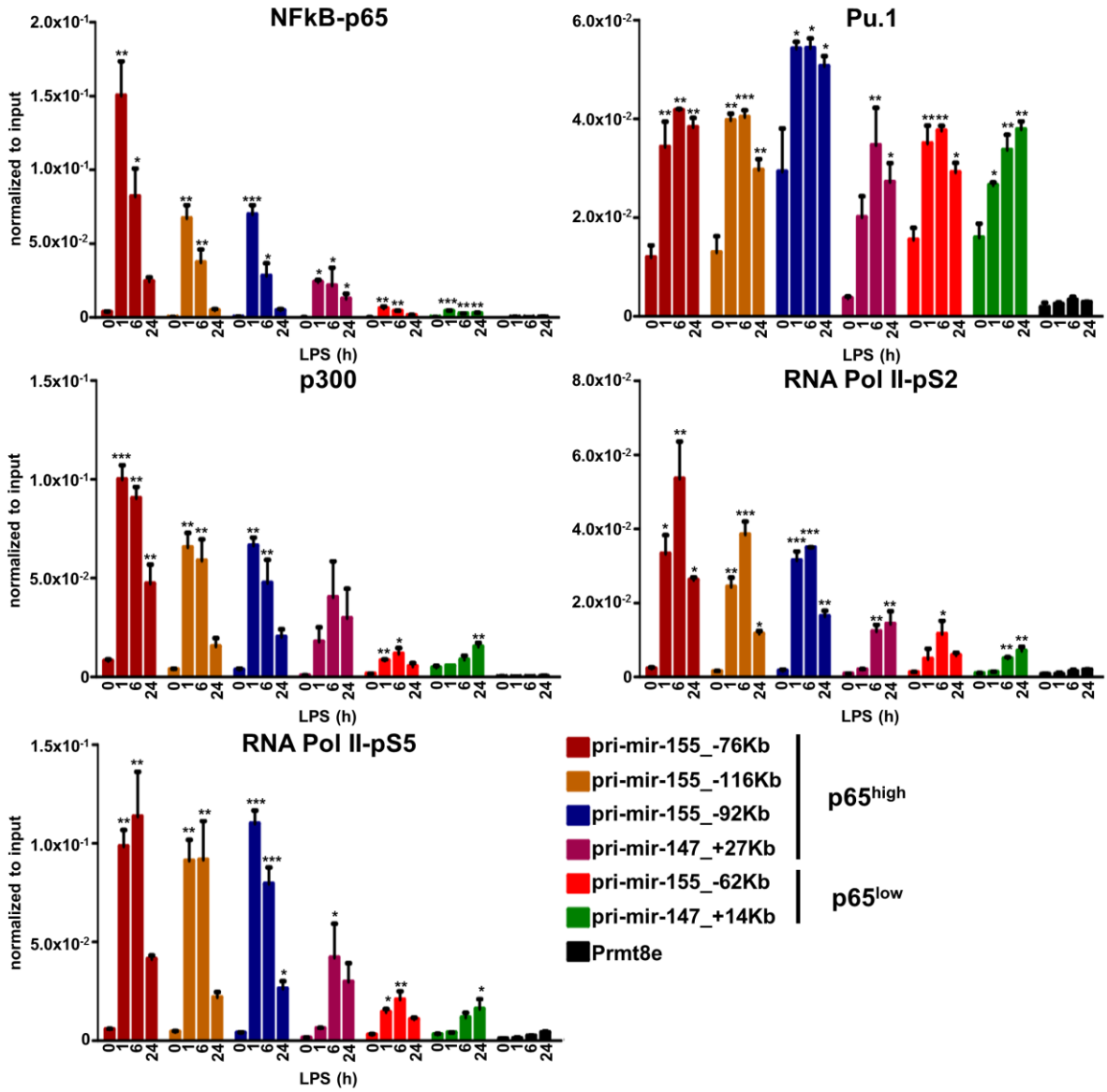

Figure 5

ACCEPTED MANUSCRIPT

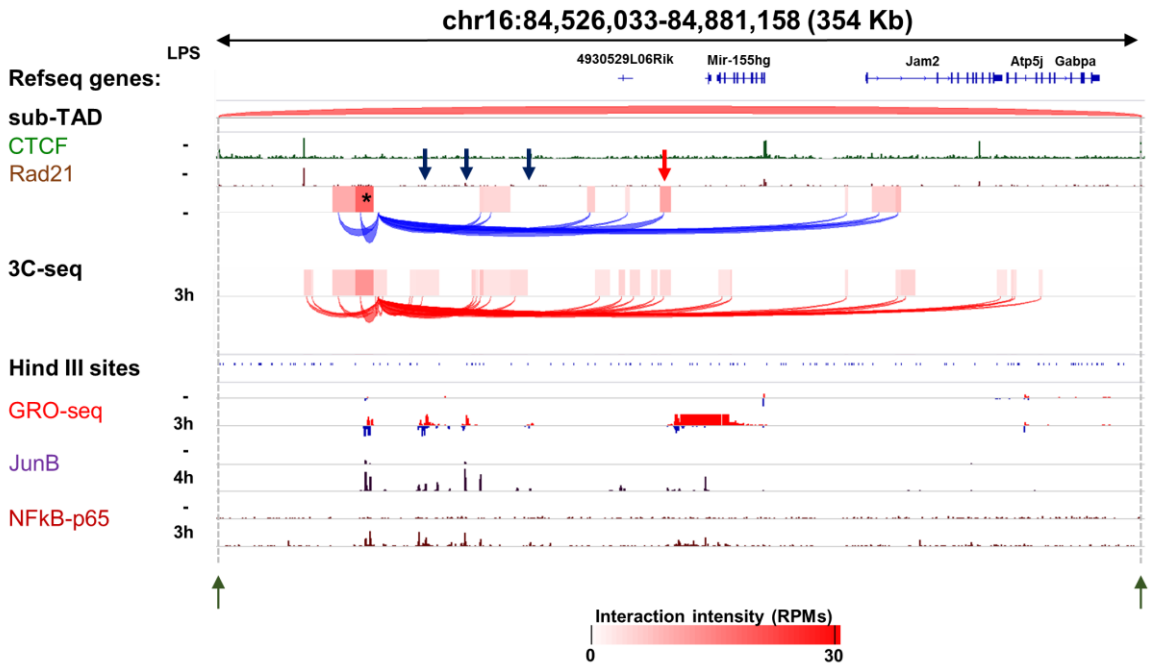

Figure 6

ACCEPTED MANUSCRIPT

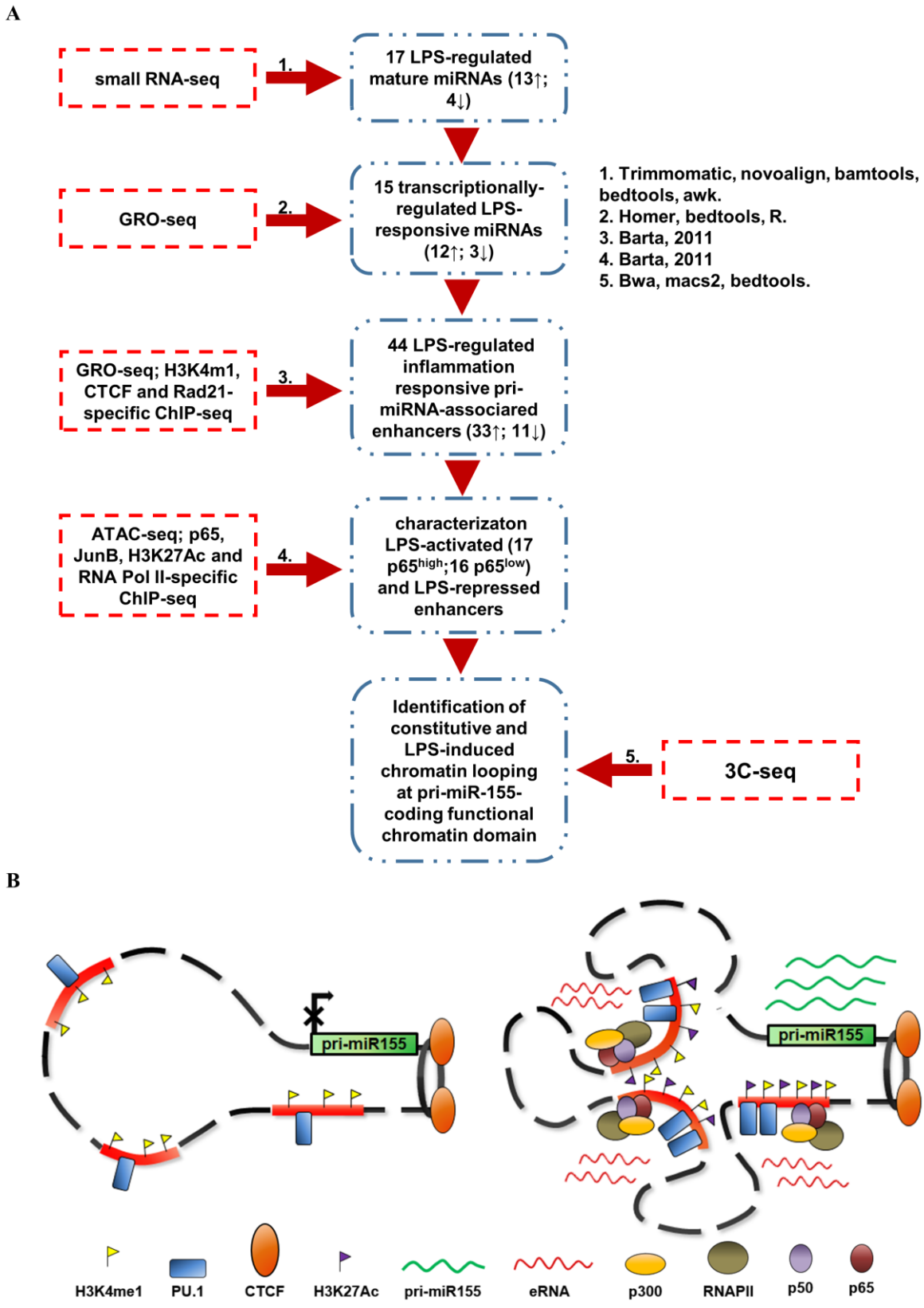

Figure 7